THE JOURNAL OF COMPARATIVE NEUROLOGY 412:17–37 (1999)

Developmental Expression of the Glycine Transporter GLYT2 in the Auditory System of Rats Suggests Involvement in Synapse Maturation

ECKHARD FRIAUF,[1]* CARMEN ARAGÓN,[2] STEFAN LÖHRKE,[1] BEATE WESTENFELDER,[1] AND FRANCISCO ZAFRA[2]

[1]Zentrum der Physiologie, University Frankfurt, Med Sch, Theodor-Stern-Kai 7, D-60596 Frankfurt, Germany

[2]Centro de Biología Molecular "Severo Ochoa," Facultad de Ciencias, Universidad Autónoma de Madrid, E-28049 Madrid, Spain

ABSTRACT

The synaptic action of many neurotransmitters is terminated by specific transporters that remove the molecules from the synaptic cleft and help to replenish the transmitter supply. Here, we have investigated the spatiotemporal distribution of the glycine transporter GLYT2 in the central auditory system of rats, where glycinergic synapses are abundant. In adult rats, GLYT2 immunoreactivity was found at all relay stations, except the auditory cortex. Many immunoreactive puncta surrounded the neuronal somata in the cochlear nuclear complex, the superior olivary complex, and the nuclei of the lateral lemniscus. In contrast, diffuse neuropil labeling was seen in the inferior colliculus and the medial geniculate body. The punctate perisomatic labeling and the diffuse neuropil labeling were very similar to the staining pattern described previously with glycine antibodies in the auditory system, suggesting that GLYT2 is a reliable marker for glycinergic synapses. However, there was a discrepancy between cytoplasmic GLYT2 and glycine labeling, as not all neuron types previously identified with glycine antibodies displayed somatic GLYT2 immunoreactivity. During development, GLYT2 immunoreactivity appeared between embryonic days 18 and 20, i.e., shortly after the time when the earliest functional synapses have been established in the auditory system. Labeling turned from a diffuse pattern to a clustered, punctate appearance. The development was also characterized by an increase of the signal intensity, which generally lasted until about postnatal day 10. Thereafter, a decrease occurred until about postnatal day 21, when the mature pattern was established in most nuclei. Because of the perinatal onset of GLYT2 immunoreactivity, we speculate that the transporter molecules participate in the process of early synapse maturation. J. Comp. Neurol. 412:17–37, 1999.

Indexing terms: cochlear nuclear complex; superior olivary complex; nuclei of the lateral lemniscus; inferior colliculus; medial geniculate body; neurotransmitter transporter

After being released from presynaptic nerve terminals, the majority of neurotransmitter types, including the amino acid and monoamine transmitters, are rapidly removed from the synaptic cleft by a high-affinity uptake machinery, thereby terminating chemical neurotransmission. The removal is accomplished by transporter proteins located in the plasma membrane of the presynaptic nerve terminals and of surrounding astroglial cells. The genes encoding the transporters for most of the major neurotrans-

Grant sponsor: Deutsche Forschungsgemeinschaft; Grant number: SFB 269; Grant sponsor: BIOMED program of the European Union; Grant number: BMH4-CT95–0571.

*Correspondence to: Eckhard Friauf, PhD, Zentrum der Physiologie, University Frankfurt, Med Sch, Theodor-Stern-Kai 7, D-60596 Frankfurt, Germany. E-mail: friauf@em.uni-frankfurt.de

Received 16 October 1998; Revised 15 April 1999; Accepted 21 April 1999

mitter types have been cloned during this decade, and several transporter families have been discovered (reviews: Uhl and Johnson, 1994; Borowsky and Hoffman, 1995; Lesch and Bengel, 1995; Malandro and Kilberg, 1996). One family comprises Na^+/Cl^--dependent carriers and includes the transporters for glycine, γ-aminobutyric acid (GABA), and catecholamines. Glycine transporters form their own subfamily of five variants (GLYT1a, GLYT1b, GLYT1c, GLYT2a, GLYT2b) cloned so far (Liu et al., 1992, 1993; Smith et al., 1992; Borowsky et al., 1993; Kim et al., 1994; Ponce et al., 1998), and GLYT1 transporters and GLYT2 transporters derive from separate genes (Guastella et al., 1992). The anatomic distribution in the central nervous system differs, as GLYT1 isoforms are distributed over wide areas in the brain, whereas GLYT2 isoforms are predominantly expressed in the spinal cord and the brainstem (e.g., Luque et al., 1995; Zafra et al., 1995a,b; Jursky and Nelson, 1996a). GLYT2 is highly correlated with strychnine-binding sites (Jursky et al., 1994; Jursky and Nelson, 1995; Luque et al., 1995), providing some anatomic evidence that it may participate in the termination of neurotransmission at classic, inhibitory glycinergic synapses.

In the present article, we studied, by light microscopy, the spatiotemporal pattern of GLYT2 expression in the central auditory system of rats. The study was performed for the following reason: inhibitory glycinergic synapses are ubiquitous in the mammalian auditory brainstem (glycine immunocytochemistry: Peyret et al., 1987; Aoki et al., 1988; Kolston et al., 1992; Henkel and Brunso-Bechtold, 1995; Winer et al., 1995; Vater, 1995; Moore et al., 1996; Vater et al., 1997; Saint Marie et al., 1997; Gleich and Vater, 1998; glycine receptor immunocytochemistry: Altschuler et al., 1986; Wenthold et al., 1988; Friauf et al., 1997; receptor binding autoradiography: Frostholm and Rotter, 1986; Sanes et al., 1987; Glendenning and Baker, 1988; Fubara et al., 1996; glycine receptor electrophysiology: Moore and Caspary, 1983; Wu and Oertel, 1986; Caspary, 1990; Wu and Kelly, 1992; Klug et al., 1995; Golding and Oertel, 1996; Koch and Grothe, 1998; Moore et al., 1998). We wanted to know whether GLYT2 proteins are also ubiquitous in auditory nuclei and present in areas where glycinergic synapses have been observed. Moreover, we asked ourselves whether GLYT2 expression starts early during ontogeny in light of our previous finding that functional glycinergic neurotransmission is present already in prenatal animals (Kandler and Friauf, 1995). Immunocytochemistry was performed from fetal to adult ages and from the auditory hindbrain to the forebrain, by using a well-characterized antiserum that detects both GLYT2a and the recently discovered GLYT2b (Zafra et al., 1995a; Ponce et al., 1998). Because the GLYT2b mRNA could be detected only after amplification with polymerase chain reaction (Ponce et al., 1998), this isoform appears to be very rare, which is why we have probably analyzed the GLYT2a isoform in the present study. Nonetheless, we refer to the neutral expression "GLYT2." Our results show that GLYT2 is heavily expressed at hindbrain and midbrain levels of the central auditory system and that the expression begins long before hearing onset and during the period of synapse maturation.

TABLE 1. Number of Animals Sampled for Each Age Group[1]

Age	E18	E20	P0	P2	P4	P8	P10	P12	P16	P22	P28	P35	Adult
No.	7	6	4	2	3	2	3	4	3	2	3	2	3

[1]E, embryonic day; P, postnatal day.

MATERIALS AND METHODS

Animals and tissue fixation

The experiments were performed on 44 Sprague-Dawley rats bred and housed in our animal facility and treated in compliance with the current German Animal Protection Law. All protocols were approved by the regional animal care and use committee (RP Darmstadt). If more than one animal was used at a given age, the animals came from at least two different litters; their ages and numbers are listed in Table 1. The day of conception and the day of birth were designated as embryonic day (E) 0 and postnatal day (P) 0, respectively; animals were considered adult when they were older than 2 months. Birth usually occurs at E21 (= P0). Postnatal animals were deeply anesthetized with chloral hydrate (600 mg/kg body weight i.p.) and perfused transcardially with 10 mM phosphate-buffered saline (PBS, pH 7.4), followed by cold Zamboni's fixative (4% paraformaldehyde and 15% saturated picric acid in PBS; pH 7.4; Somogyi and Takagi, 1982). Fetal animals were delivered by means of cesarean section from deeply anesthetized, time-pregnant dams and perfused with the above fixative. After perfusion, brains were removed and post-fixed in the fixative for 3 hours and then cryoprotected in a 30% sucrose/PBS solution overnight in the refrigerator.

Staining and analysis

Coronal sections were cut at 50 µm on a freezing microtome, collected in PBS, and immunocytochemistry was performed on these free-floating sections to visualize the GLYT2 protein. To do so, sections were blocked with nonimmune goat serum and immunolabeled for the antigen by using an overnight incubation in the refrigerator with the primary antibody (rabbit anti-GLYT2; 0.5 µg/ml; for specificity, e.g., lack of cross-reactivity with GLYT1 proteins, see Zafra et al., 1995a). The next day, the sections were incubated in the biotinylated secondary antibody for 90 minutes (goat anti-rabbit IgG (H+L)-BIOT, 1:200; Southern Biotechnology Associates, Birmingham, AL) and in the avidin-biotin-horseradish peroxidase reagent for 90 minutes (Vectastain Elite kit, 1:100, Vector Laboratories, Burlingame, CA), both at room temperature. The reaction product was developed in the presence of 0.01% hydrogen peroxide by using 3,3′-diaminobenzidine tetrahydrochloride as the substrate (0.05%, Sigma, Deisenhofen, Germany). All antibodies were diluted in PBS containing 1.5% (v/v) normal goat serum and 1% (w/v) bovine serum albumins, and 0.3% Triton X-100 was added to the solutions in animals older than P7 to permeabilize the tissue. The sections were mounted on gelatinized slides, allowed to dry, dehydrated in alcohol, and mounted in Entellan (Merck, Darmstadt, Germany). Controls in which the primary antibody was omitted confirmed the specificity of the immunolabeling. Labeled sections were analyzed with brightfield and Nomarski optics by using a Zeiss Axioscope (Zeiss, Göttingen, Germany) equipped with Plan-Neofluar

lenses (5×–100×), and photomicrographs were taken on Kodak TMax100 film. Some sections were digitized with the Zeiss Axioscope equipped with a 12-bit cooled CCD camera (C4742–95–12NR, Hamamatsu, Japan), processed with Adobe Photoshop software, and printed on a Kodak XLS 8650 PS dye-sublimation printer (cf. Fig. 1A, Fig. 11A–C).

Methodologic considerations

In the developmental series, the staining intensity was evaluated. Because such developmental evaluations can lead to inaccurate conclusions, we had to consider some potential pitfalls. First, as mentioned above, we took into account that litter-specific peculiarities can occur; we, therefore, obtained age-matched rat pups from at least two different litters. Second, because the sections from the 44 animals were stained in separate sessions and during a period that extended over several months, we had to consider that the staining intensity may have been affected by changes in the quality of antibodies, by seasonal variations, or both. Fortunately, however, we found no evidence of such variability. Instead, age-related properties in the staining intensity were consistently obvious, regardless of whether the sections were treated in the same staining session or not. Also, we found no evidence that variations in fixation might have drastically influenced the staining intensity. Third, we obtained nine brains from animals between P8 and P12 (see Table 1) to make sure that we analyzed enough material for the conclusion that the peak intensity occurred during that period. Finally, we analyzed brain structures other than the auditory system to determine the time at which peak intensity occurred. This step was done because peak intensity occurred at around P10 in most auditory nuclei and because of the possibility that antibody penetration of the tissue and/or antigen binding might have been best at that time. However, in the cerebellum, peak intensity did not occur at around P10; rather, we observed a relatively weak signal at this age and a steady increase thereafter, indicating that the peak seen in the auditory nuclei reflected the natural development and that it was not caused by methodologic factors.

RESULTS

GLYT2 immunoreactivity in the adult auditory system

The distribution of GLYT2 immunoreactivity (GLYT2-ir) in the central auditory system of adult rats is illustrated in Figures 1–4 and summarized in Figure 5. Except for the auditory cortex, GLYT2-ir was present at all levels of the auditory pathway, i.e., from the cochlear nuclear complex (CN) up to the medial geniculate body (MGB). However, labeling intensity in the brainstem nuclei was much higher than in the diencephalon. Therefore, we will focus on the brainstem nuclei in the following, whereas only a brief account will be attributed to the MGB.

In the CN, strong GLYT2-ir occurred in the dorsal cochlear nucleus (DCN, Fig. 1A) and the anteroventral cochlear nucleus (AVCN, Fig. 1C), whereas the posteroventral cochlear nucleus (PVCN) contained less immunoreactivity (Fig. 1A,B). In all three nuclei, a punctate staining pattern was obvious. Within the DCN, the central, cell-dense fusiform cell layer showed a stronger signal than the superficial molecular layer or the underlying deep layer (Fig. 1A), consistent with the reported high glycine concentration in the fusiform cell layer (Godfrey et al., 1997). In the PVCN, the octopus cell area (oca) was almost devoid of labeling, whereas the multipolar cell area (mca; cf. Osen, 1969) was more heavily labeled (Fig. 1A,B). The granular region of the PVCN appeared to be very weakly labeled (Fig. 1A). Cytoplasmic labeling of some scattered neurons in the PVCN was evident even at low magnification (Fig. 1B), and at higher magnification, it became obvious that these GLYT2-ir neurons were located amongst immunonegative somata (Fig. 2A). Because of their location and paucity, it is likely that these GLYT2-ir neurons are stellate cells of the glycine-ir subtype described by others, i.e., presumptive interneurons providing inhibitory input to the DCN and VCN (Cant, 1981; Wenthold et al., 1987; Oertel et al., 1990; Oertel and Wickesberg, 1993; Nelken and Young, 1994; Ferragamo et al., 1998). Regardless of whether they were immunopositive or immunonegative, most PVCN neurons were densely covered with GLYT2-ir puncta, which surrounded the soma perimeter. A similar subcellular pattern of GLYT2-ir puncta was seen in the DCN (Fig. 2B) and the AVCN (Fig. 2C), including the entry zone of the 8th nerve (Fig. 2D). In these areas, the majority of somata were immunonegative, yet surrounded by densely stained puncta. Often, the stumps of the primary dendrites were also decorated with GLYT2-ir puncta (e.g., Fig. 2C,D).

Cytoplasmic staining of DCN neurons was not easily detectable; it was restricted to a few oval-shaped cells located in the deep layer, close to the medioventral border of the nucleus (not shown). Due to their location, shape, and size (ca. 15 μm × 12 μm), these GLYT2-ir cells possibly represent tuberculoventral neurons (Wenthold et al., 1987; Saint Marie et al., 1991; Wickesberg et al., 1991; Oertel and Wickesberg, 1993; Zhang and Oertel, 1993b). No other neuron type in the DCN displayed cytoplasmic staining for GLYT2; for instance, we found no evidence for GLYT2-ir in cartwheel cells, neurons that are labeled with antibodies to glycine conjugates (e.g., Wenthold et al., 1987; see Discussion for further references) and that probably provide inhibitory input to DCN fusiform and giant cells (Godfrey et al., 1997; Golding and Oertel, 1997). In the AVCN, immunoreactive somata were present in caudal aspects, whereas rostral aspects appeared to be devoid of cytoplasmic labeling (Fig. 1C); few immunoreactive somata occurred in the cochlear root nucleus (CRN).

In the superior olivary complex (SOC; Fig. 3), GLYT2-ir was obvious in all nuclei analyzed, i.e., the lateral superior olive (LSO), the medial superior olive (MSO), the superior paraolivary nucleus (SPN), the medial nucleus of the trapezoid body (MNTB), the ventral nucleus of the trapezoid body (VNTB), and the lateral nucleus of the trapezoid body (LNTB). The intensity of the signal varied, with the LSO and SPN displaying the highest, the MSO an intermediate, and the MNTB, LNTB, and VNTB the lowest levels (Fig. 3A). Like in the CN, GLYT2-ir was mostly located around immunonegative somata and proximal dendrites, and it occurred in a punctate pattern in the SPN (Fig. 3B), the LSO (Fig. 3C), the MSO (Fig. 3E), the LNTB (Fig. 3F), and the VNTB (not shown). In contrast, most, if not all, MNTB neurons displayed cytoplasmic labeling of their somata, whereas GLYT2-ir puncta were only rarely seen (Fig. 3D). The cytoplasmic labeling pat-

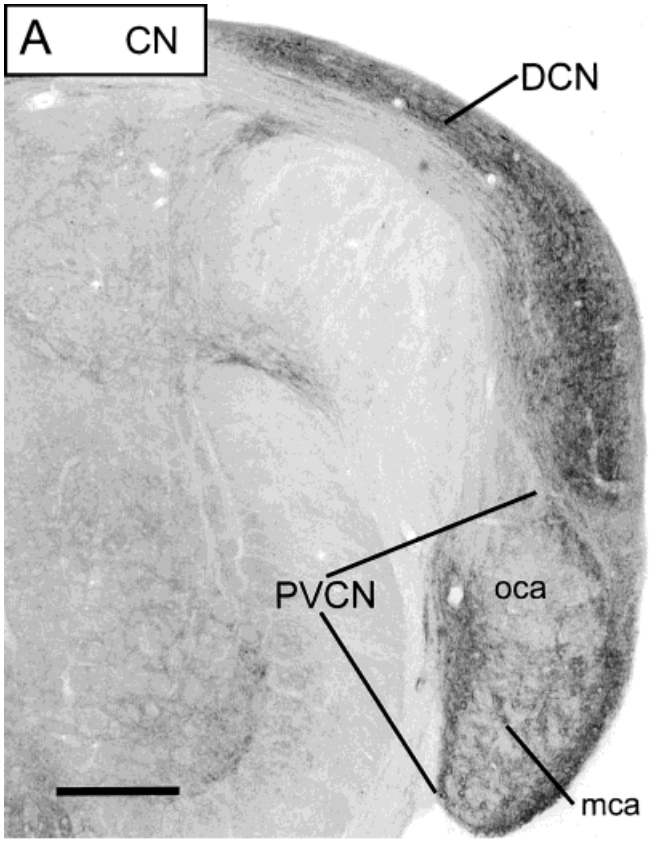

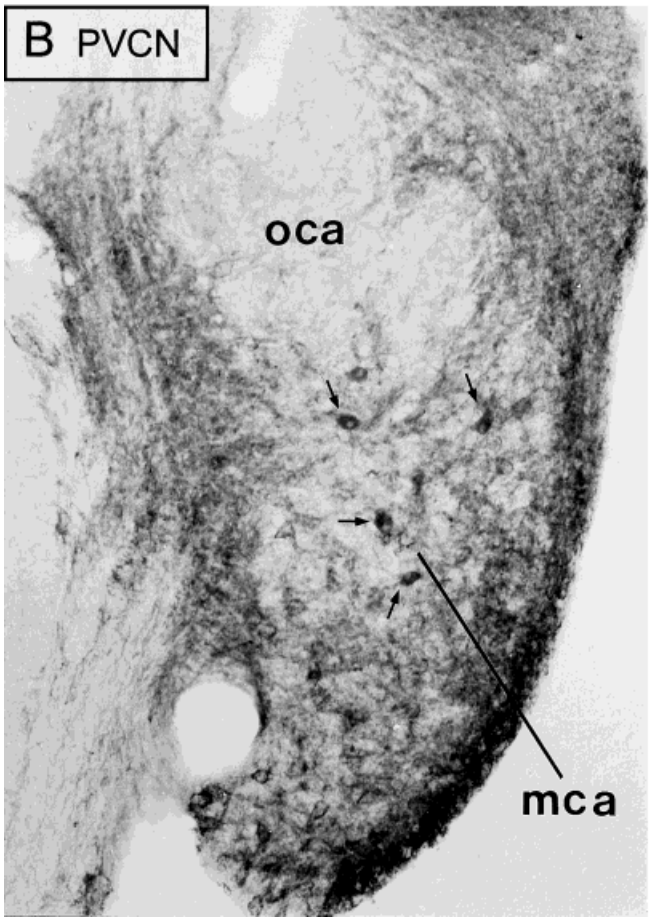

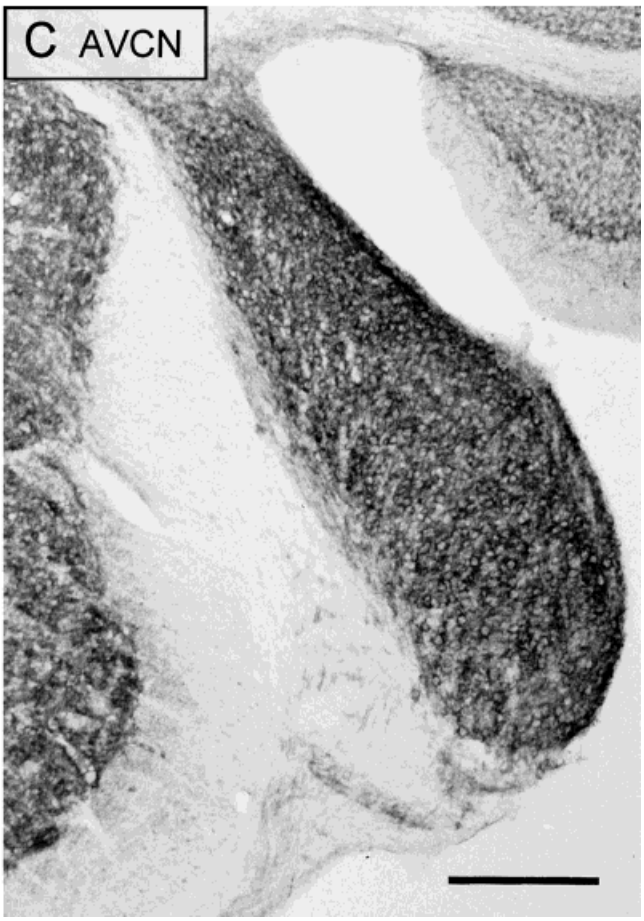

Fig. 1. Photomicrographs of coronal sections through the cochlear nuclear complex (CN) of adult rats, immunostained for the high-affinity glycine transporter protein GLYT2. **A:** Dorsal cochlear nucleus (DCN) and caudal posteroventral cochlear nucleus (PVCN). **B:** PVCN. **C:** Anteroventral cochlear nucleus (AVCN). Note heavy immunoreactivity in all CN nuclei, particularly in the DCN and AVCN. In the PVCN, the octopus cell area (oca) is almost devoid of labeling (A and B) and several neurons in the multipolar cell area (mca) display cytoplasmic labeling (arrows in B). In this and all subsequent figures, dorsal is toward the top and lateral is to the right. Scale bar in C = 400 μm in A; 300 μm in C; 200 μm in B.

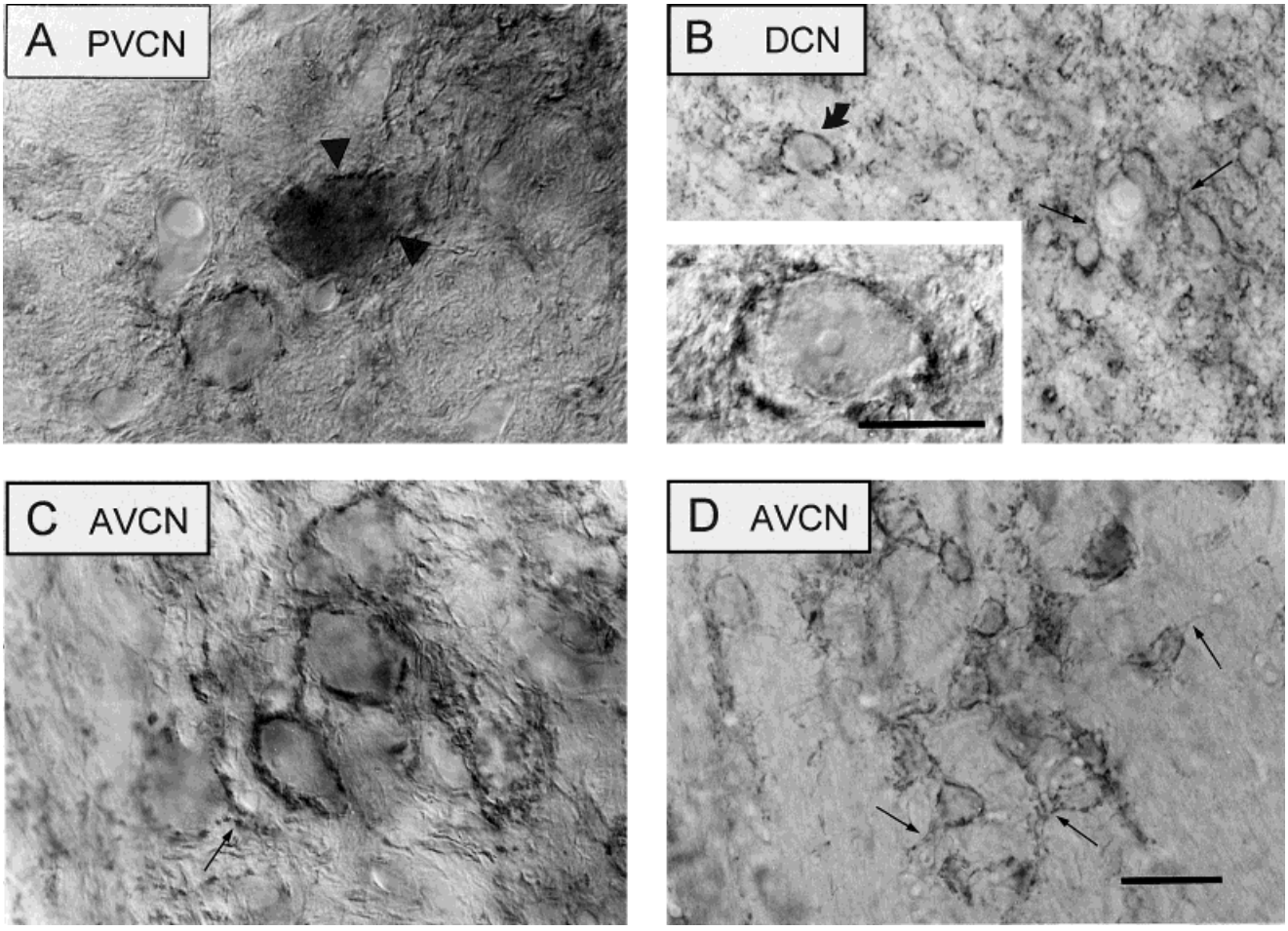

Fig. 2. High-magnification photomicrographs showing GLYT2 immunoreactivity in the CN of adult rats. **A:** Posteroventral cochlear nucleus (PVCN), multipolar cell area; Nomarski optics. **B:** Dorsal cochlear nucleus (DCN), curved arrow points to the neuron depicted in the inset at higher magnification and photographed with Nomarski optics. **C:** Anteroventral cochlear nucleus (AVCN), spherical cell area; Nomarski optics. **D:** AVCN at 8th nerve entry. In all subdivisions of the CN, immunoreactive structures are densely incrusting immunonegative neurons. Labeling is characterized by clusters of heavily labeled puncta outlining the somata and proximal dendrites (arrows in B–D). In the multipolar cell area of the PVCN (A), immunonegative and immunopositive neurons (cytoplasmic labeling) are located in close vicinity to each other. Note that the soma of the immunopositive neuron in A is also decorated with immunoreactive puncta (arrowheads). Scale bar in D = 20 μm in A,C; 50 μm in B,D; in inset = 20 μm.

tern of MNTB neurons, which we identified as principal neurons because of their oval perikarya and the eccentric location of their nuclei (Morest, 1968; Kuwabara and Zook, 1991), is in line with the observation that these cells are glycinergic (Aoki et al., 1988; Bledsoe et al., 1990; Henkel and Brunso-Bechtold, 1995), providing a major inhibitory input to other SOC nuclei and to the nuclei of the lateral lemniscus (Bledsoe et al., 1990; Kuwabara and Zook, 1992; Sommer et al., 1993; Schofield, 1994). A subpopulation of VNTB neurons displayed cytoplasmic labeling, and these neurons were also incrusted by perisomatic puncta (not shown), resembling the situation in the PVCN. With the exception of MNTB and VNTB neurons, no other neuron population in the SOC displayed a cytoplasmic signal.

Each of the three nuclei of the lateral lemniscus, the dorsal, intermediate, and ventral (DNLL, INLL, and VNLL, respectively), displayed GLYT2-ir. There was a dorsoventral gradient in the staining level, with the VNLL showing the strongest signal (Fig. 4A) and the DNLL showing the weakest. Again, labeling occurred around immunonegative somata in most cases, such that numerous immunopositive puncta were seen along the soma perimeter (Fig. 4C). A small number of VNLL neurons displayed cytoplasmic labeling, whereas no INLL or DNLL somata were stained (not shown).

In the inferior colliculus (IC; Fig. 4B,D), the labeling pattern differed considerably from that seen in the other brainstem nuclei. Immunoreactive signal around a neuronal soma perimeter was rarely seen; rather diffuse labeling occurred in the neuropil and appeared to be homogeneously distributed within the central nucleus (Fig. 4D). Amongst the three major subdivisions of the adult IC (central [CIC], dorsal cortex [DCIC], external cortex [ECIC]), the DCIC contained the highest amount of GLYT2-ir (Fig. 4B). Cytoplasmic labeling was not observed in the IC.

Rostral to the midbrain, GLYT2-ir was generally low in all brain regions, which goes along with previous findings (Zafra et al., 1995a; Goebel, 1996). The MGB contained a few faintly labeled fibers, which were more prominent in

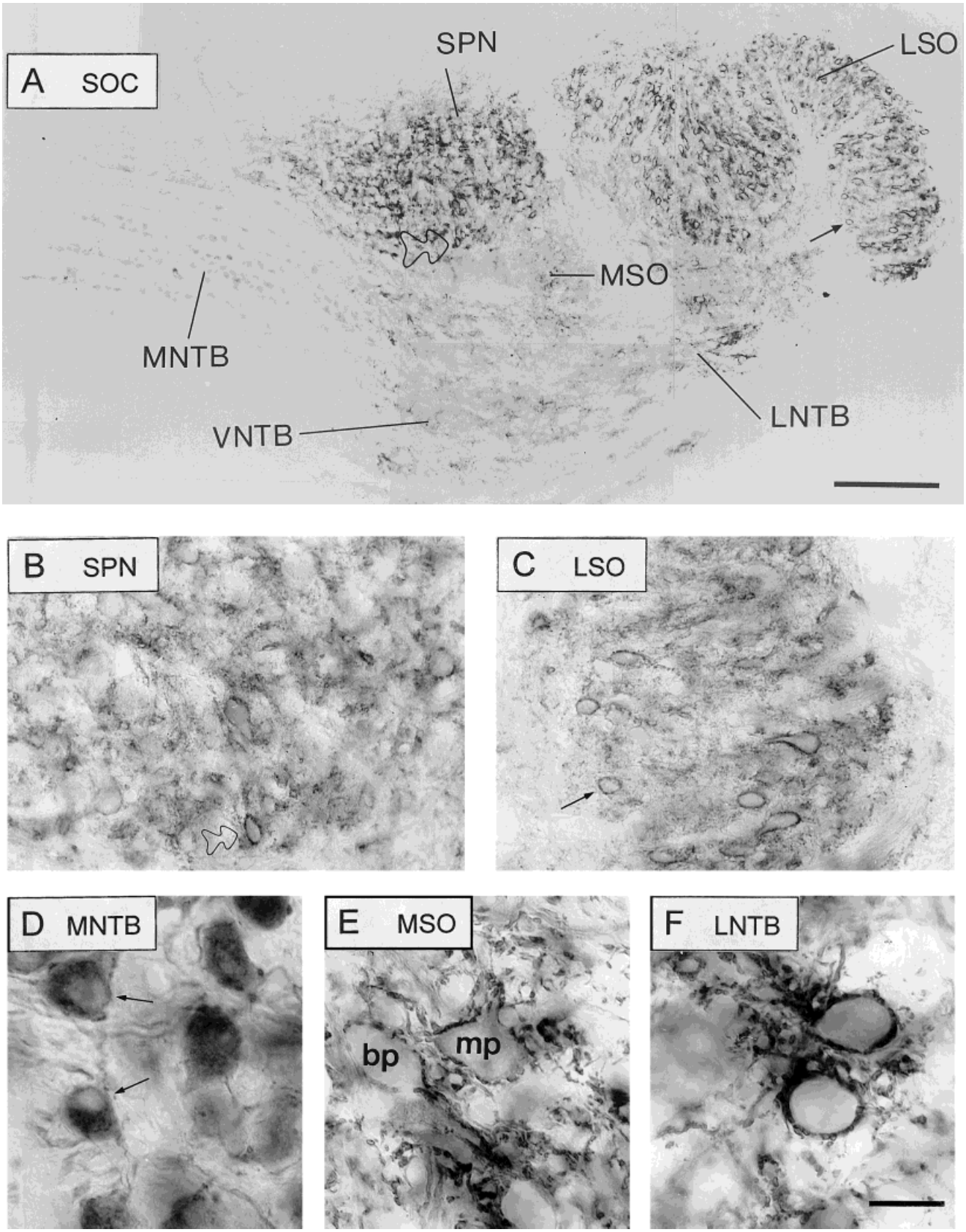
A SOC
SPN
LSO
MSO
MNTB
LNTB
VNTB
B SPN
C LSO
D MNTB
E MSO
bp
mp
F LNTB

Figure 3

medial than in lateral aspects (not shown). No GLYT2-ir was detected in the auditory cortex. A schematic summary of the distribution of GLYT2 in the auditory brainstem nuclei of the adult rat is illustrated in Figure 5.

GLYT2 immunoreactivity in the developing auditory system

The distribution of GLYT2-ir in the central auditory system of developing rats is illustrated in Figures 6–11 and summarized in Figure 12. As detailed information on the spatiotemporal changes of GLYT2 is provided in the legends to these figures, we will concentrate on some general aspects in the following chapters to avoid unnecessary repetition. In general, GLYT2-ir appeared around birth in all auditory brainstem nuclei. Although no labeling was seen at E18, the cytoplasm of MNTB neurons had become intensely immunoreactive by E20. At P4, all brainstem nuclei displayed GLYT2-ir; the immunosignal appeared last in the DCN, namely between P2 and P4 (Fig. 12). At the subcellular level, labeling turned from an originally diffuse pattern into a clustered, punctate appearance. In the majority of brainstem nuclei, this process took place during the first postnatal week. The gross labeling pattern in the medullary and pontine nuclei (CN, SOC, NLL) resembled that seen in adults around P8, yet further modifications were seen at the subcellular level (GLYT2-ir puncta became more crisp) and in the staining intensity (it decreased after the peak signal had occurred at around P10; Fig. 12). The adult-like pattern in the medullary and pontine nuclei was reached after about 3 weeks postnatal, both at the regional and the subcellular level.

At no age did we observe any transient labeling in an area which was devoid of GLYT2-ir in the adult, i.e., the oca of the PVCN. Likewise, cytoplasmic labeling during brain maturation was found only in those nuclei that displayed such a signal in adult rats as well (i.e., PVCN [Fig. 6K–M], MNTB [Figs. 7, 8A–D], VNTB [Fig. 9E–H], VNLL [Fig. 10G–K]), indicating that those auditory neurons that are GLYT2 immunonegative in the adult do not transitorily synthesize a detectable amount of transporter molecules during development. The cytoplasmic signal in these nuclei appeared quickly and early, i.e., before birth, demonstrating that synthesis of GLYT2 molecules begins about 2 weeks before hearing onset (at P12; Jewett and Romano, 1972; Uziel et al., 1981; Geal-Dor et al., 1993) and shortly after the time when the earliest functional synapses have been established (Wu and Oertel, 1987; Sanes, 1993; Kandler and Friauf, 1995).

Development of GLYT2-ir in the IC began early, as evidenced by the fact that a strong signal was present already at P0 in ventral aspects of the CIC (Fig. 11A). Subsequently, labeling progressed into more dorsal regions, such that neuropil in the whole CIC was heavily GLYT2-ir at P10 (Fig. 11B). Thereafter, labeling intensity decreased, but the DCIC and the ECIC became also labeled by P22, although still quite weakly (Fig. 11C). After P22, the signal intensity in the DCIC and ECIC increased further. Because this remodeling process took more than 10 days, development in the IC lasted beyond 3 weeks postnatal, thus lagging behind that in the medullary nuclei, which obtained their adult-like pattern at around P21. The adult-like pattern, characterized by the highest amount of GLYT2-ir being present in dorsal aspects of the DCIC, was obtained around P28.

In the MGB, GLYT2-ir fibers were first seen at about P21. They were present at the same site as in adults. No major age-dependent changes occurred thereafter, except for a slight increase in the number and labeling intensity. The adult-like situation was seen at about 4 weeks postnatal. In the auditory cortex, no GLYT2-ir was seen at any age investigated (not shown).

Taken together, GLYT2-ir appears early in the maturing central auditory system of the rat (Fig. 12). The development is characterized by an initial increase of the labeling intensity, followed by a decrease after P10. Clustering into punctate, perisomatic signals occurs in all nuclei except the IC and MGB. By the end of the 4th postnatal week, the mature pattern is acquired, both at the subcellular and the supracellular level. Thus, the spatiotemporal development is remarkably similar to that described for the inhibitory glycine receptor (GlyR; Friauf et al., 1997).

DISCUSSION

Three major results emerge from this study: First, the glycine transporter GLYT2 is abundant in all auditory brainstem nuclei of the adult rat (Fig. 5) and found in those areas where glycinergic synapses have been described previously. Second, there is a discrepancy between cytoplasmic labeling for GLYT2 and glycine, in that all GLYT2-ir somata almost certainly correspond to glycinergic neurons described previously, yet not all cell types determined to be glycinergic by other authors are also GLYT2-ir. Third, GLYT2 expression in the auditory system begins before, or shortly after, birth in rats (Fig. 12), and thus during the period of synapse formation, indicating that the transporter molecules may be involved in maturation processes.

GLYT2 appears to be a reliable marker for glycinergic synapses

The spatial expression pattern of GLYT2 in the central auditory system, as determined here, is in accordance with results from previous studies which provided a survey throughout the central nervous system of mice and rats, both in the adult animal (Jursky and Nelson, 1995; Luque et al., 1995; Zafra et al., 1995a) and during development (Zafra et al., 1995b; Jursky and Nelson, 1996a), thereby supplying fragmentary information on the auditory system. We found GLYT2-ir in those auditory areas in which inhibitory, strychnine-sensitive glycinergic synapses have

Fig. 3. GLYT2 immunoreactivity (-ir) in the superior olivary complex (SOC) of adult rats. **A:** Low-power photomicrograph (montage) showing strong immunoreactivity in the lateral superior olive (LSO) and the superior paraolivary nucleus (SPN) and lower levels in the medial superior olive (MSO) and the ventral and lateral nuclei of the trapezoid body (VNTB and LNTB). Cytoplasmic labeling is only seen in the medial nucleus of the trapezoid body (MNTB). B–F: High-power photomicrographs of different SOC nuclei, illustrating similarities and differences in the labeling pattern. **B:** Center of the SPN (open arrows in A and B point to the same neuron). Labeling is seen around somata and in the neuropil. **C:** Lateral limb of the LSO (arrows in A and C point to the same neuron). Bipolar cells are densely incrusted by immunoreactive puncta and neuropil labeling is similar to that in the SPN. **D:** Central aspects of the MNTB. GLYT2-ir is present in virtually all principal neurons, which can be identified by their shape and their eccentric nuclei (arrows). **E:** MSO. Perisomatic labeling appears around bipolar (bp) and multipolar (mp) neurons. **F:** LNTB. The density of puncta around immunonegative somata is particularly high in this nucleus. Compared with MSO neurons, there is a nearly continuous arrangement of the puncta. Scale bar = 240 μm in A; in F = 50 μm for B,C; 20 μm for D–F.

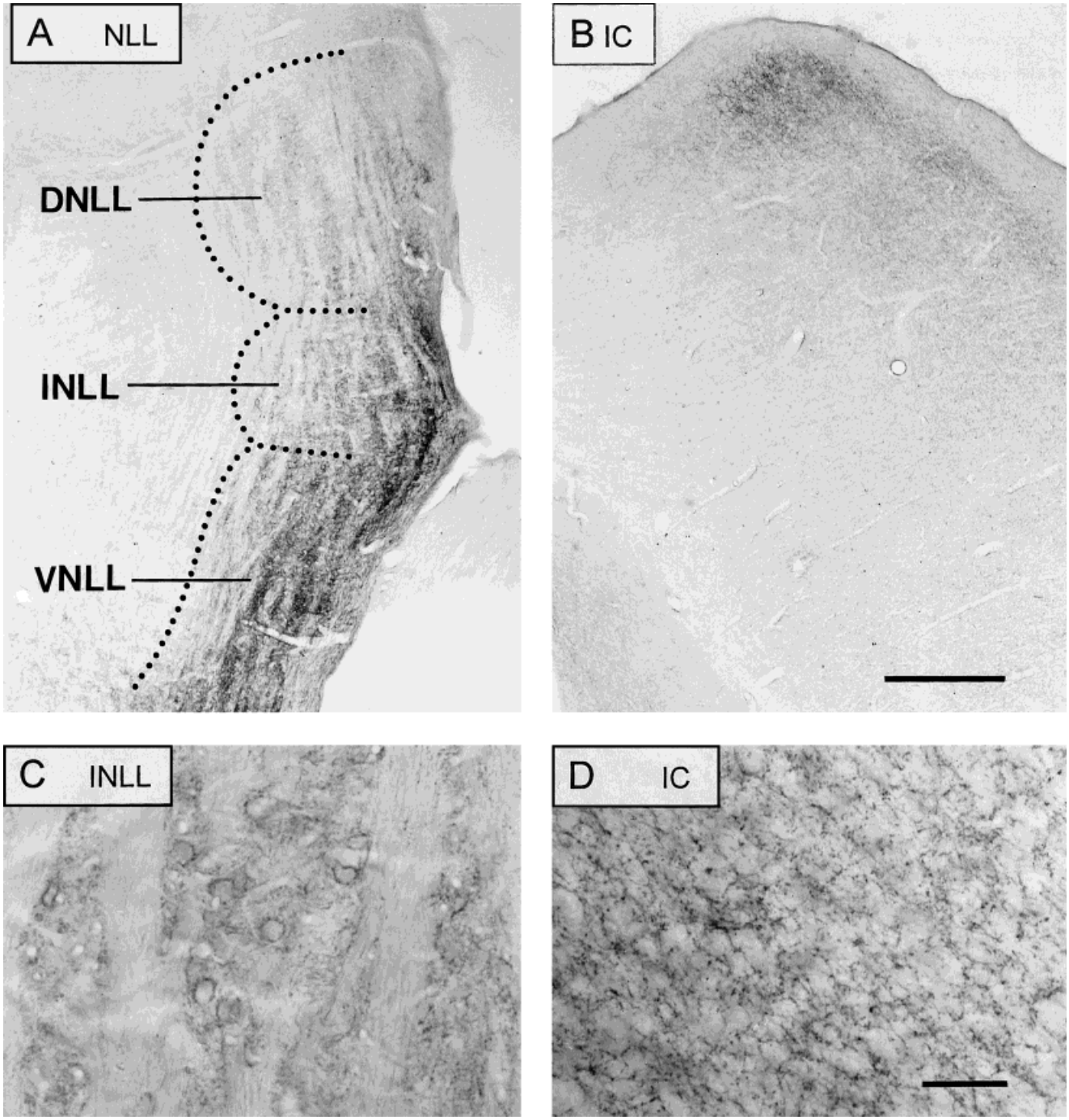

Fig. 4. GLYT2 immunoreactivity (-ir) in the nuclei of the lateral lemniscus (NLL) and the inferior colliculus (IC) of adult rats. **A:** NLL with the three subdivisions: dorsal (DNLL), intermediate (INLL), and ventral (VNLL). Labeling is heaviest in the VNLL, intermediate in the INLL, and relatively weak in the DNLL. **B:** IC. GLYT2-ir is highest in the dorsal cortex. At this low magnification, immunoreactivity in the central nucleus can barely be seen. **C:** INLL at higher magnification. Note perisomatic staining around most neurons. **D:** Central subdivision of the IC at high magnification, showing that GLYT2 labeling is evenly distributed within the neuropil and not clustered around somata, which is in contrast to all other auditory brainstem nuclei. Scale bars = 400 μm in B (applies to A,B); 50 μm in D (applies to C,D).

been described earlier (see below for references). Moreover, we found that the punctate staining pattern corresponds very well to that seen for glycine-ir terminals or for the distribution of 1 GlyR subunits. For example, in the CN, we observed GLYT2-ir puncta, presumably representing axon terminals, around immunonegative somata in all areas, except for the oca of the PVCN. Our findings are in agreement with published results on glycine-ir in the CN, describing a stronger signal in the DCN than in the PVCN (Aoki et al., 1988; Wickesberg et al., 1991), and literature therein), the highest level of [^{3}H]strychnine-binding within the DCN occurring in the fusiform cell layer (Willott et al.,

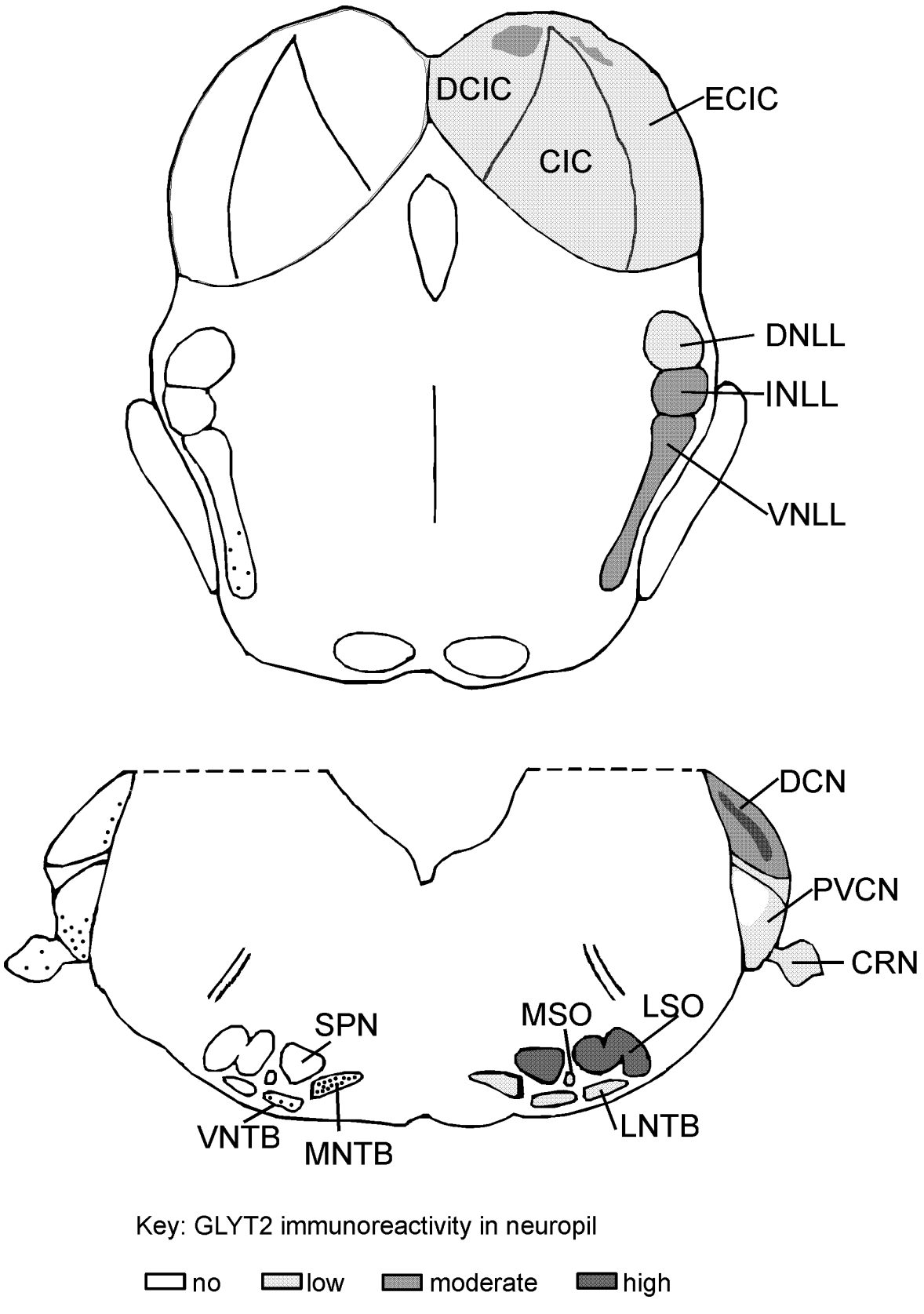

Fig. 5. Summary of GLYT2 immunoreactivity in the auditory brainstem nuclei of the adult rat. Neurons and neuropil (presumptive axonal endings) are depicted on the left and right side, respectively. The neuronal density reflects their relative concentration, and the gray areas reflect the relative intensity of labeled neuropil. CIC, central subdivision of the inferior colliculus; CRN, cochlear root nucleus; DCIC, dorsal cortex of the inferior colliculus; DCN, dorsal cochlear nucleus; DNLL, dorsal nucleus of the lateral lemniscus; ECIC, external cortex of the inferior colliculus; INLL, intermediate nucleus of the lateral lemniscus; LNTB, lateral nucleus of the trapezoid body; LSO, lateral superior olive; MNTB, medial nucleus of the trapezoid body; MSO, medial superior olive; PVCN, posteroventral nucleus of the cochlear nucleus; SPN, superior paraolivary nucleus; VNLL, ventral nucleus of the lateral lemniscus; VNTB, ventral nucleus of the trapezoid body.

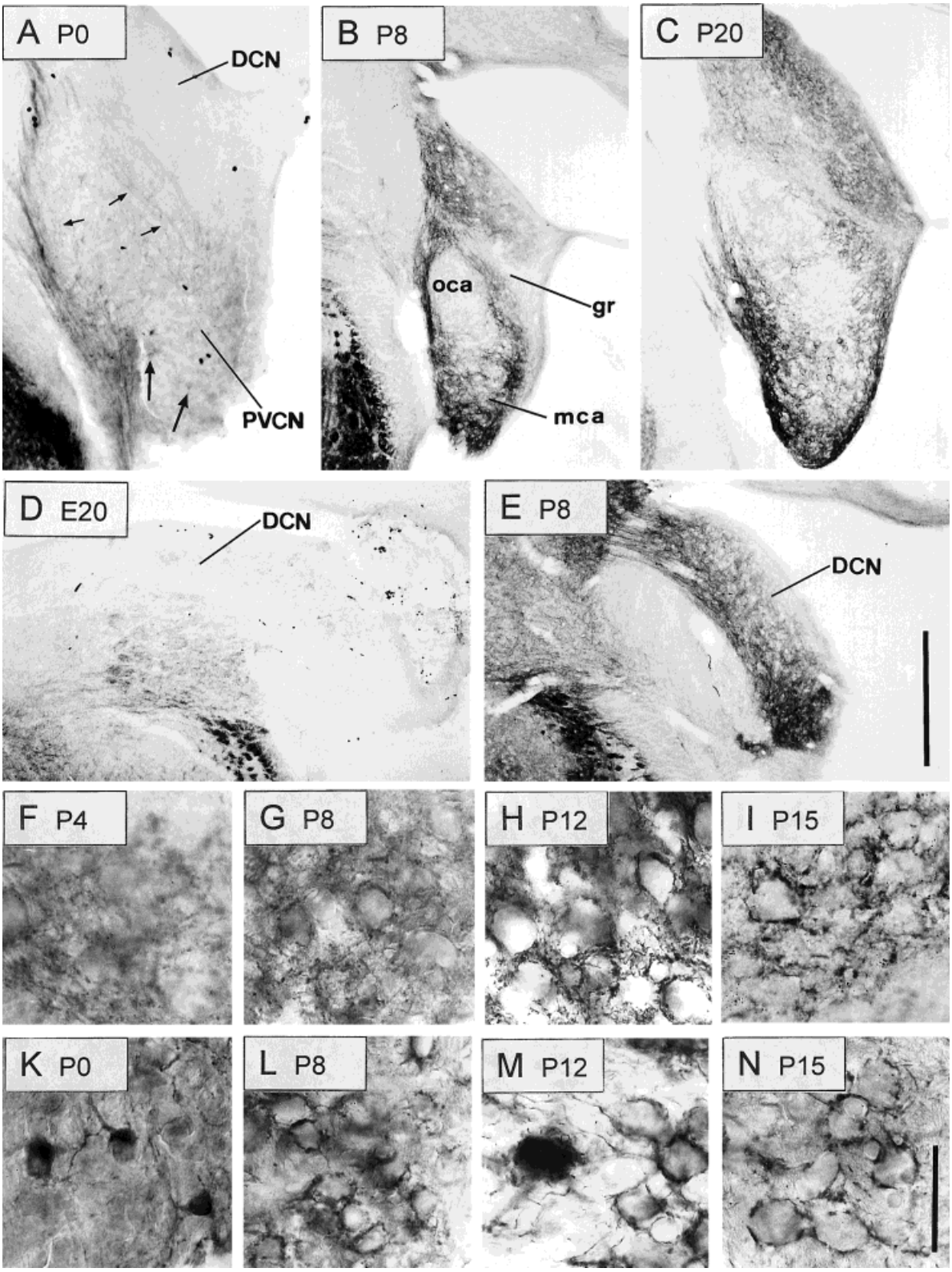

Fig. 6. Development of GLYT2-immunoreactivity in the cochlear nucleus. **A–E:** Overviews of the posteroventral cochlear nucleus (PVCN) and dorsal cochlear nucleus (DCN) at low magnification. **F–I:** DCN at high magnification. **K–N:** PVCN at high magnification. Until the day of birth (postnatal day (P) 0), the DCN is still unstained (A,D); at P0, labeling in the PVCN is weak and found in fibers (A, small arrows) and several neuronal somata (K). These somata are located in the ventromedial portion of the PVCN (A, large arrows). At P8, heavy labeling is observed in the multipolar cell area (mca), whereas the octopus cell area (oca) and the granular region (gr) are almost devoid of labeling (B). Most neurons in the mca show perisomatic labeling at this age (L). In the DCN, labeling is diffuse until P8 (B, E–G), when some neuronal somata become outlined by reaction product (G). Between P8 and P15, labeling becomes more crisp and immunoreactive puncta appear around the somata in the DCN (H,I) and the PVCN (M,N). At both P12 (H,M) and P15 (I,N), proximal dendrites are also covered with reaction product. Cytoplasmic staining of PVCN neurons is present throughout development (K,M). The adult-like pattern, characterized by crisp, punctate staining, is achieved by P20 (C). Scale bar in E = 200 μm in A; 400 μm for B–E; in N = 40 μm in F–N.

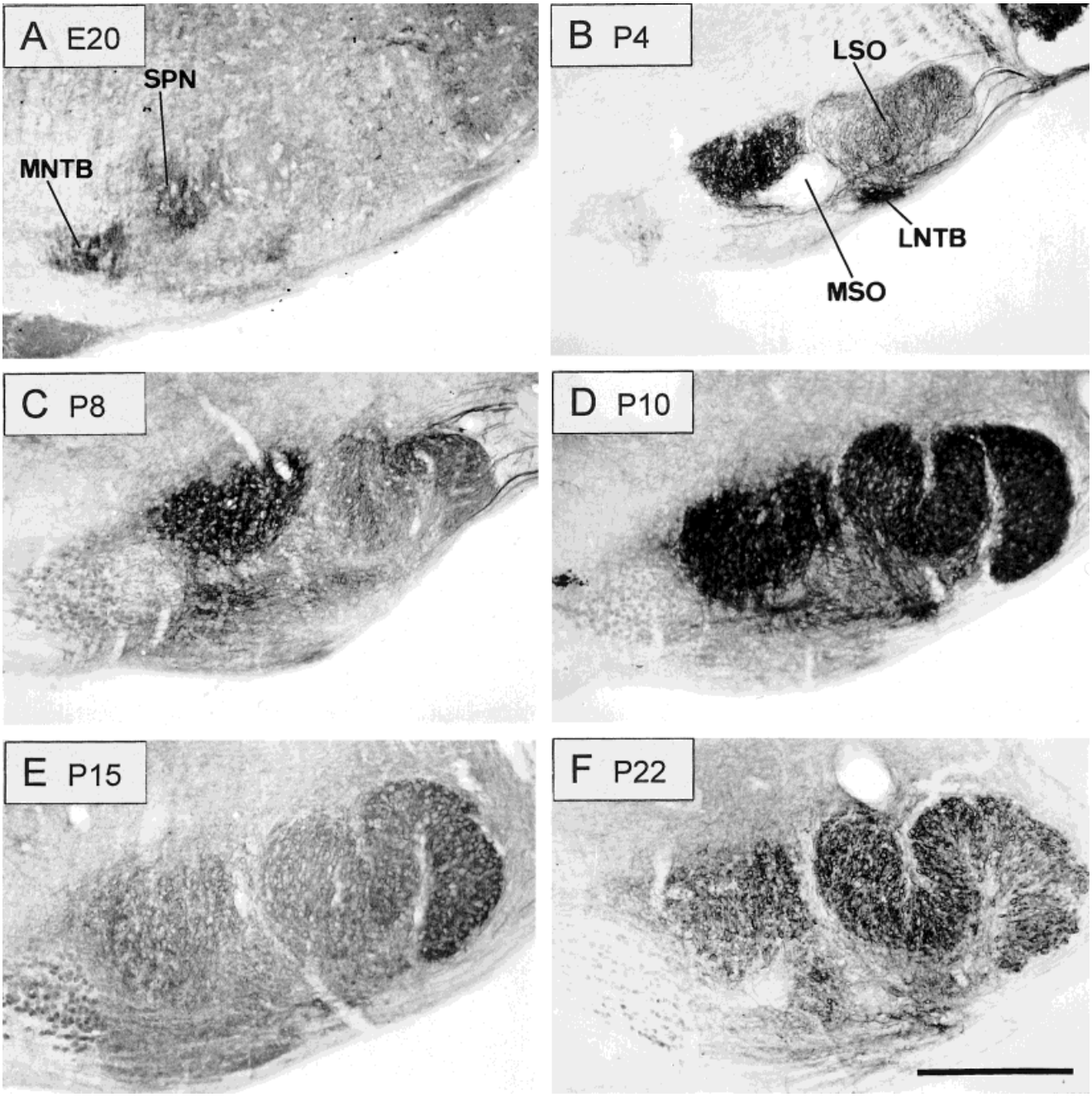

Fig. 7. Development of GLYT2 immunoreactivity (-ir) in the superior olivary complex (SOC). **A:** At embryonic day (E) 18, no SOC nucleus displays a signal, but the MNTB is strongly labeled by E20. Aside from the MNTB, the SPN is also clearly labeled before birth (A). **B:** By P4, labeling intensity in the SPN has increased, and the LSO has also become clearly immunoreactive. There is also a strong signal in the LNTB, whereas the MSO seems to be unstained at low magnification (cf. Fig. 8B, however, for a high-mag photograph). **C:** At P8, GLYT2-ir is present in all SOC nuclei, with the highest intensity being present in the SPN. **D:** Immunoreactivity peaks at around P10, when the SPN and the LSO are very intensely labeled. **E:** By P15, labeling intensity has decreased considerably, and (**F**) the adult-like pattern has appeared by P22. Abbreviations as in Figure 5. Scale bar = 400 μm in F (applies to A–F).

1997), a punctate pattern around unlabeled cell bodies in the AVCN (Wenthold et al., 1987; Kolston et al., 1992), and a paucity of labeled structures in the oca of the PVCN (Wickesberg et al., 1991; Kolston et al., 1992; Moore et al., 1996).

A high similarity between the punctate, pericellular staining pattern seen for GLYT2 on the one hand and for glycine on the other was not only present in the CN, but also in the SOC nuclei (LSO: Wenthold et al., 1987; Helfert et al., 1989,1992; MNTB, MSO, and SPN: Helfert et al., 1989) and the nuclei of the lateral lemniscus (Aoki et al., 1988). This similarity between GLYT2 and glycine labeling was also obvious in the IC, where a homogeneous neuropil labeling, rather than perisomatic puncta, appears for both

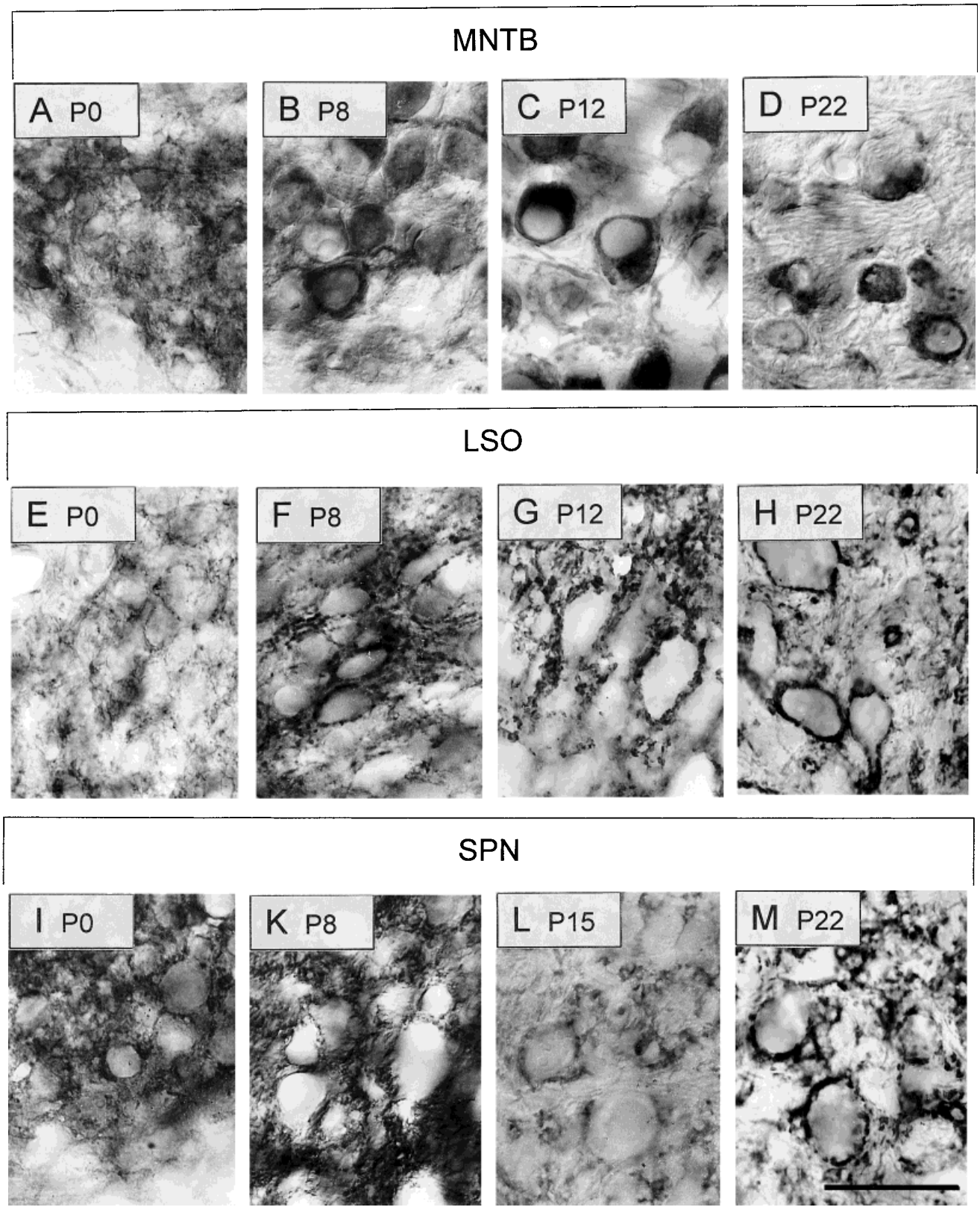

Fig. 8. High-magnification photomicrographs illustrating the development of GLYT2 immunoreactivity (-ir) in the medial nucleus of the trapezoid body (MNTB) (**A–D**), the lateral superior olive (LSO) (**E–H**), and the superior paraolivary nucleus (SPN) (**I–M**). Until P0 (A), neuropil labeling in the MNTB is heavy, contributing to the strong signal illustrated in Figure 6A. Cytoplasmic staining in MNTB principal cells (note their eccentric nuclei, which lack GLYT2-ir) is present at all successive ages (B–D). In the LSO, diffuse labeling is obvious in perinatal animals (E), turning into clustered labeling around spindle-shaped somata until P8 (F). Clustering proceeds during further development (G,H); cytoplasmic GLYT2-ir is never observed in the LSO. The labeling pattern of the SPN is similar to that seen in the LSO, yet labeling of the neuropil appears to be more intense during the first postnatal week (I,K). By P15 (L), punctate labeling around immunonegative somata is obvious, and at P22 (M), the labeling pattern is very reminiscent of that in the LSO (cf. panel H) and cannot be distinguished from that in the adult. Scale bar = 40 μm in M (applies to A–M).

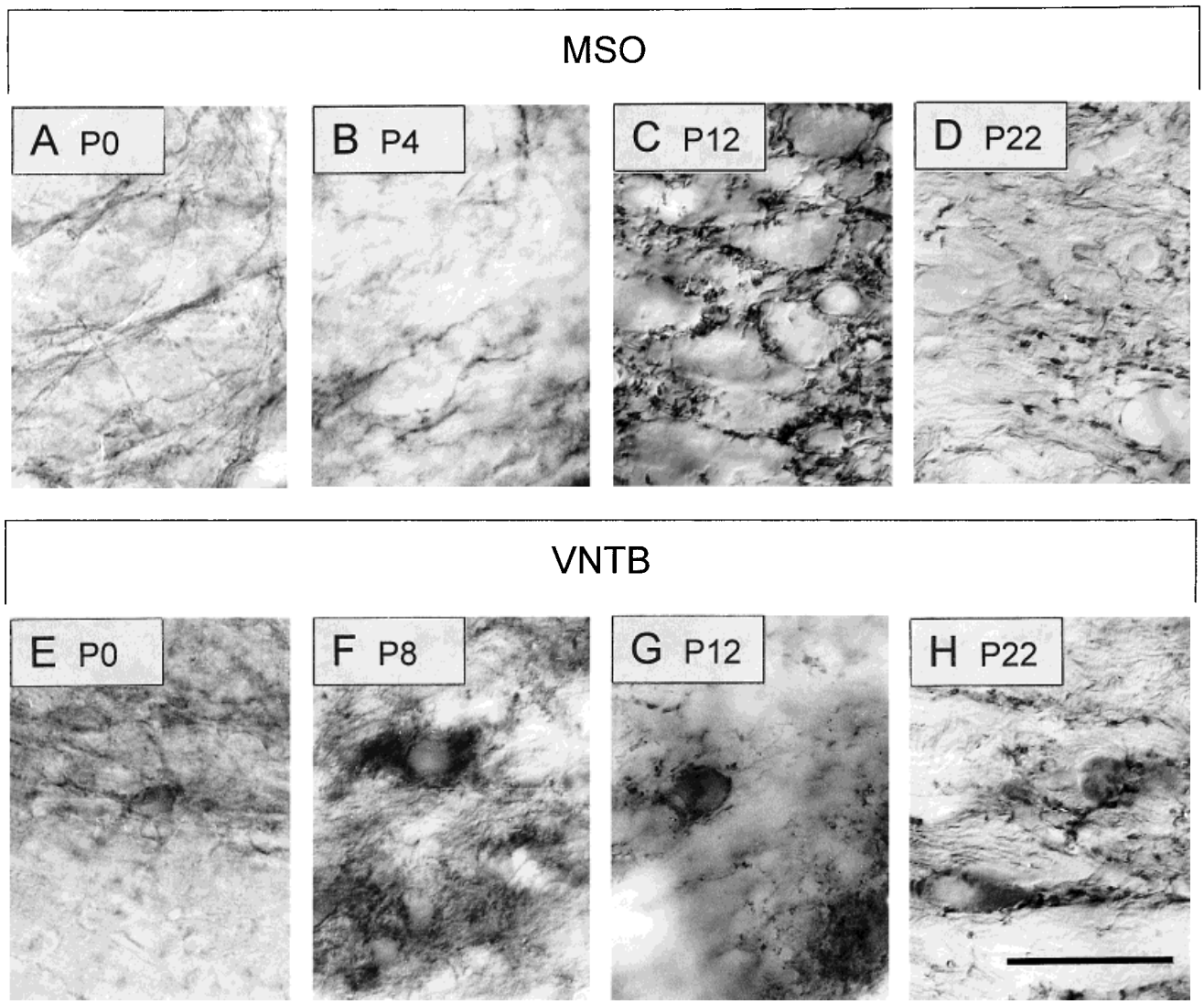

Fig. 9. High-magnification photomicrographs illustrating the development of GLYT2 immunoreactivity (-ir) in the medial superior olive (MSO) (**A–D**) and the ventral nucleus of the trapezoid body (VNTB) (**E–H**). Until postnatal day(P) 4 (A,B), GLYT2-ir in the MSO is weak and restricted to the neuropil, presumably to traversing fibers. By P12 (C), punctate staining around MSO somata has become quite intense. Labeling intensity decreases thereafter, yet the punctate staining pattern remains (D). In the VNTB, some faint somatic labeling occurs at P0 (E) and increases during the first postnatal week (F). By P12 (G), immunoreactive somata can be identified which themselves are covered with GLYT2-ir puncta. This labeling pattern is maintained until P22 (H), when the adult-like pattern has been achieved. Scale bar = 40 μm in H (applies to A–H).

molecules (Aoki et al., 1988). Because of the similarity in the noncytoplasmic staining patterns found with GLYT2-ir and glycine-ir, we conclude that GLYT2-ir can be used to stain glycinergic synapses in the auditory system (see also Poyatos et al., 1997). Our conclusion is corroborated by the fact that 1 subunits of the GlyR (Jursky and Nelson, 1995; Friauf et al., 1997) appear to be distributed in the same manner as GLYT2 transporters. Double-labeling studies are necessary to provide final proof that GLYT2 and GlyR molecules are indeed codistributed.

Discrepancy between cytoplasmic labeling for GLYT2 and glycine

Concerning the cytoplasmic labeling pattern, our data about GLYT2 only partly parallel those reported for the distribution of glycine-ir somata in the auditory system. A coincidence was observed in the PVCN (Aoki et al., 1988; Kemmer and Vater, 1997), the MNTB (Wenthold et al., 1987; Aoki et al., 1988; Helfert et al., 1989), and the VNTB (Wenthold et al., 1987; Helfert et al., 1989; Saint Marie et al., 1993; Ostapoff et al., 1997). Furthermore, the absence of GLYT2-ir somata in the DNLL, the IC, the MGB, and the auditory cortex is also in line with the absence of glycine-ir neurons in these areas (Aoki et al., 1988; Winer et al., 1995; Saint Marie et al., 1997). However, in the DCN, we found only a small number of GLYT2-ir somata and those were located in the deep layer, probably corresponding to tuberculoventral neurons (e.g., Oertel and Wickesberg, 1993). This finding contrasts with the often reported abundance of glycine-ir neurons in the superficial

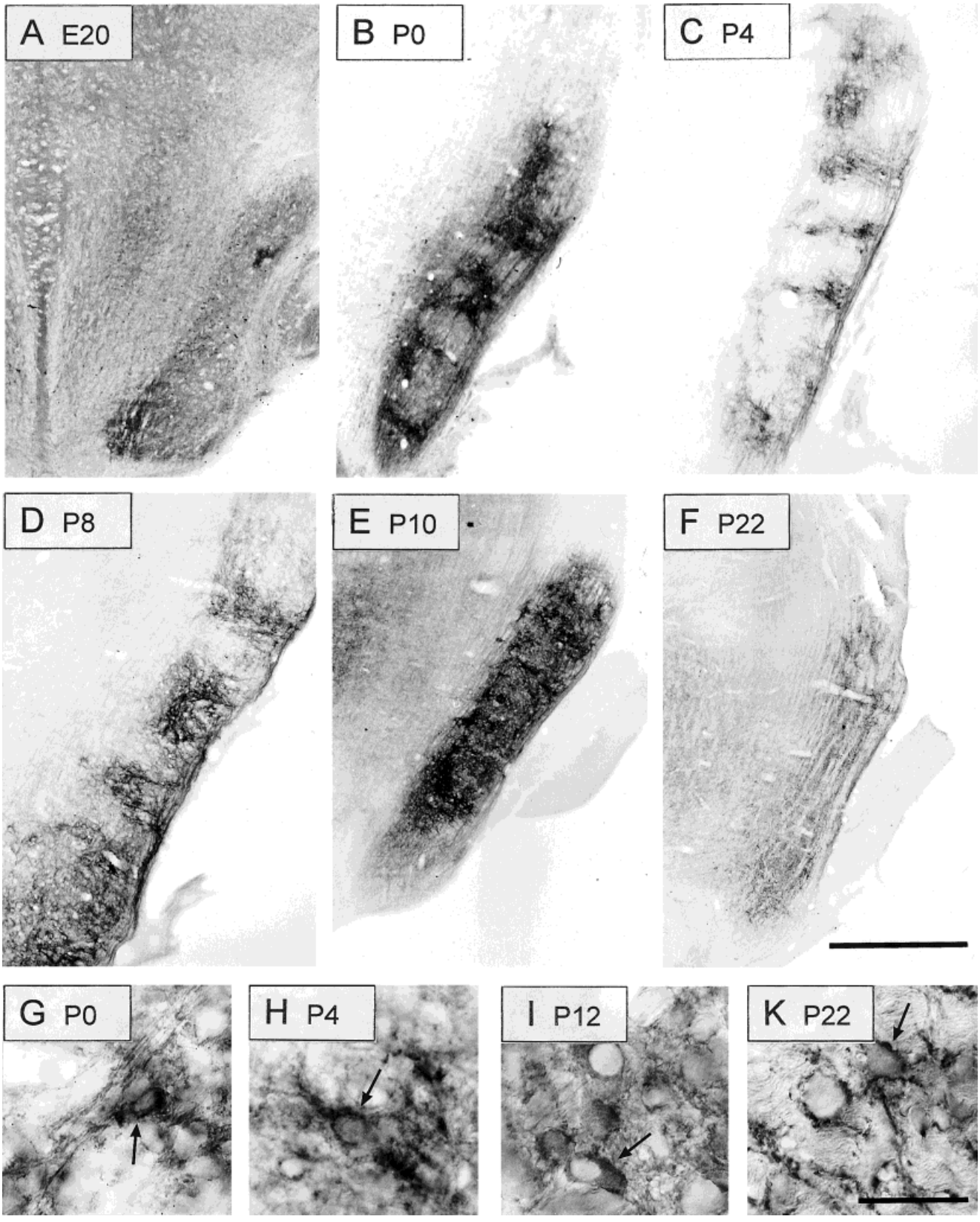

Fig. 10. Development of GLYT2 immunoreactivity in the NLL. **A–F:** Low-magnification photomicrographs of the VNLL. **G–K:** High-magnification photomicrographs of the VNLL. At embryonic day (E)20 (A), diffuse labeling is present throughout the VNLL, and the ventral-most regions appear particularly intensely labeled. By birth (B), the labeling pattern has become more discrete and repetitively organized, horizontal bands can be discerned. These bands remain present until postnatal day (P) 8 (C,D), yet they cannot be distinguished from background after P10 (E,F). Labeling peaks at around P10 (E) and the adult-like labeling pattern becomes present by P22 (F). Cytoplasmic labeling of VNLL neurons is present at all ages tested (G–K, arrows), yet the intensity of the signal appears to decline with age. Punctate staining around the cell bodies and proximal dendrites develops only during the second and third postnatal weeks. Scale bar in F = 400 μm for A–D; 800 μm for E,F; in K = 40 μm for G–K.

layers of the DCN (Aoki et al., 1988; Winer et al., 1995; Riggs et al., 1995; Kemmer and Vater, 1997; Gleich and Vater, 1998), which most likely are cartwheel and stellate cells (Wenthold et al., 1987; Osen et al., 1990; Saint Marie et al., 1991; Kolston et al., 1992; Gates et al., 1996; Golding and Oertel, 1997). A similar situation is present in the VNLL, where only few somata stain for GLYT2, although the majority of VNLL neurons display glycine-ir (Saint Marie et al., 1997). Lastly, we found no cytoplasmic GLYT2 labeling in the LSO, which differs from the scattered cell labeling seen with glycine immunocytochemistry in a variety of species (Wenthold et al., 1987; Helfert et al., 1989; Saint Marie et al., 1989; Vater, 1995). Together these results show that GLYT2-ir in the cytoplasm is almost certainly associated with a glycinergic phenotype, but not all glycinergic neurons are also somatically labeled for GLYT2.

What could be the reason for the discrepancy between cytoplasmic GLYT2 and cytoplasmic glycine labeling? One possible explanation is that it is due to species-specific differences. Indeed, with the exception of the papers by Aoki et al. (1988) and Gates et al. (1996), whose findings are based on rats, all other aforementioned reports were obtained in different species (guinea pig, hamster, gerbil, cat, mustache bat). Nevertheless, this does not explain the diverse results found in rats, and because the pattern of glycinergic axon terminals and GLYT2-ir puncta is remarkably similar, even across species, we think that species-specific differences are unlikely (see, however, Winer et al., 1995; Moore et al., 1996, for accounts on qualitative and quantitative interspecies differences). A second explanation is that GLYT2 expression is not strictly related to a glycinergic transmitter phenotype. This would contradict the recent finding, based on cultured spinal neurons, that the glycine transporter GLYT2 is a reliable marker for glycine-immunoreactive neurons (Poyatos et al., 1997). In fact, in the retina and the cerebellum, it appears that GLYT2 gene expression in presynaptic neurons is not associated with inhibitory glycine receptors in postsynaptic neurons (Goebel, 1996), providing some indirect evidence that GLYT2 transporters and glycine transmitter molecules are not imperatively colocated in the same synaptic terminal. Interestingly, the GLYT1 transporter type is found in glycinergic neurons of the retina, and it is possible that GLYT1 transporters also occur in those glycinergic auditory neurons in which we have not observed GLYT2-ir, herein fulfilling the task of neurotransmitter uptake. Second, it should be mentioned that the amino acid glycine is involved in metabolic aspects other than neurotransmission (Daly and Aprison, 1982; Daly, 1990) and, therefore, glycine-ir must not necessarily suggest a glycinergic transmitter phenotype. However, because glycinergic neurotransmission has been demonstrated in several physiologic in vitro studies after stimulation of presumptive glycinergic neurons, it is very likely that the glycine-ir neurons in the auditory brainstem indeed use glycine as a transmitter (CN: Wu and Oertel, 1986; Wickesberg and Oertel, 1990; Zhang and Oertel, 1993a, 1994; Golding and Oertel, 1996, 1997; Ferragamo et al., 1998; SOC: Sanes and Rubel, 1988; Kandler and Friauf, 1995; Smith, 1995; Wu and Kelly, 1995; NLL: Wu and Kelly, 1996). Third, it has been shown for tuberculoventral and cartwheel cells that cytoplasmic glycine-ir is modulated by experimental manipulations affecting neural activity (Wickesberg et al., 1994). But because it is unknown whether GLYT2-ir can also be increased or decreased in response to stimulation, it is unclear whether a specific modulation of glycine-ir accounted for our finding of less cytoplasmic labeling for GLYT2 than for glycine. A fourth explanation is that GLYT2 molecules and glycine transmitter molecules are indeed colocated, not only in the axon terminals but also in the cytoplasm, yet the intracellular GLYT2 concentration in some neurons (DCN, LSO, VNLL) was too low to be above the detection threshold achieved with our method. Such a low concentration could be the result of a slow rate of synthesis, an efficient sorting of the protein into the axons, and/or a fast transport into the axonal periphery. A slow rate of synthesis is unlikely, however, in light of results obtained with in situ hybridization experiments, showing a very high level of GLYT2 mRNA in the DCN and the VNLL (Luque et al., 1995). Thus, it is most likely that we underestimated the population of auditory glycinergic neurons with our GLYT2 immunocytochemistry.

GLYT2 may participate in the process of synapse maturation

With the exception of the MGB, GLYT2-ir appeared perinatally in the rat central auditory system. For example, ventral aspects of the CIC displayed a strong signal in the neuropil already at P0, at a time when axon collaterals and terminal arbors from CN neurons are still being formed in this region (Kandler and Friauf, 1993). Likewise, glycinergic neurotransmission in the LSO undergoes substantial functional modifications (rat: Kandler and Friauf, 1995; Ehrlich et al., 1998a,b; gerbil: Sanes, 1993; Kotak et al., 1998) at the time when GLYT2 molecules are being expressed. Thus, GLYT2 is present at a time when early synaptic maturation processes take place, indicating that the transporter may participate in these developmental processes. In addition, GLYT2-ir begins to appear when the "adult" GlyR isoform, characterized by the presence of $\alpha 1$ subunits, has not yet been synthesized (Friauf et al., 1997). Instead, the "neonatal" isoform, characterized by the presence of $\alpha 2$ subunits (Betz, 1991), is expressed in the auditory system of fetal and newborn rats (Piechotta et al., 1998). This finding is again indicative of a very early role of GLYT2 transporters during the development of glycinergic synapses.

An early expression has also been reported for other neurotransmitter transporters, namely the GABA transporter subtypes GAT1-GAT4 (Jursky and Nelson, 1996b; Howd et al., 1997) and the glutamate transporter GLAST (Ullensvang et al., 1997). Because of the early expression, the authors have concluded that the transporters may be connected with the maturation of the GABAergic inhibitory and the glutamatergic excitatory system, respectively.

Interestingly, functional glycinergic neurotransmission has been shown recently to be required for the clustering of "neonatal" GlyRs: blockade of the neurotransmission by the glycine-antagonist strychnine inhibited the accumulation of receptor molecules (Kirsch and Betz, 1998; Levi et al., 1998). It is conceivable that an optimal concentration of glycine is necessary for proper maturation and that GLYT2 molecules participate in the regulation of this concentration, thus enabling appropriate activation of GlyRs. This theory again suggests an involvement of the GLYT2 transporter in synapse maturation. Finally, it must be considered that glycine exerts depolarizing effects during early development in SOC neurons of neonatal rats

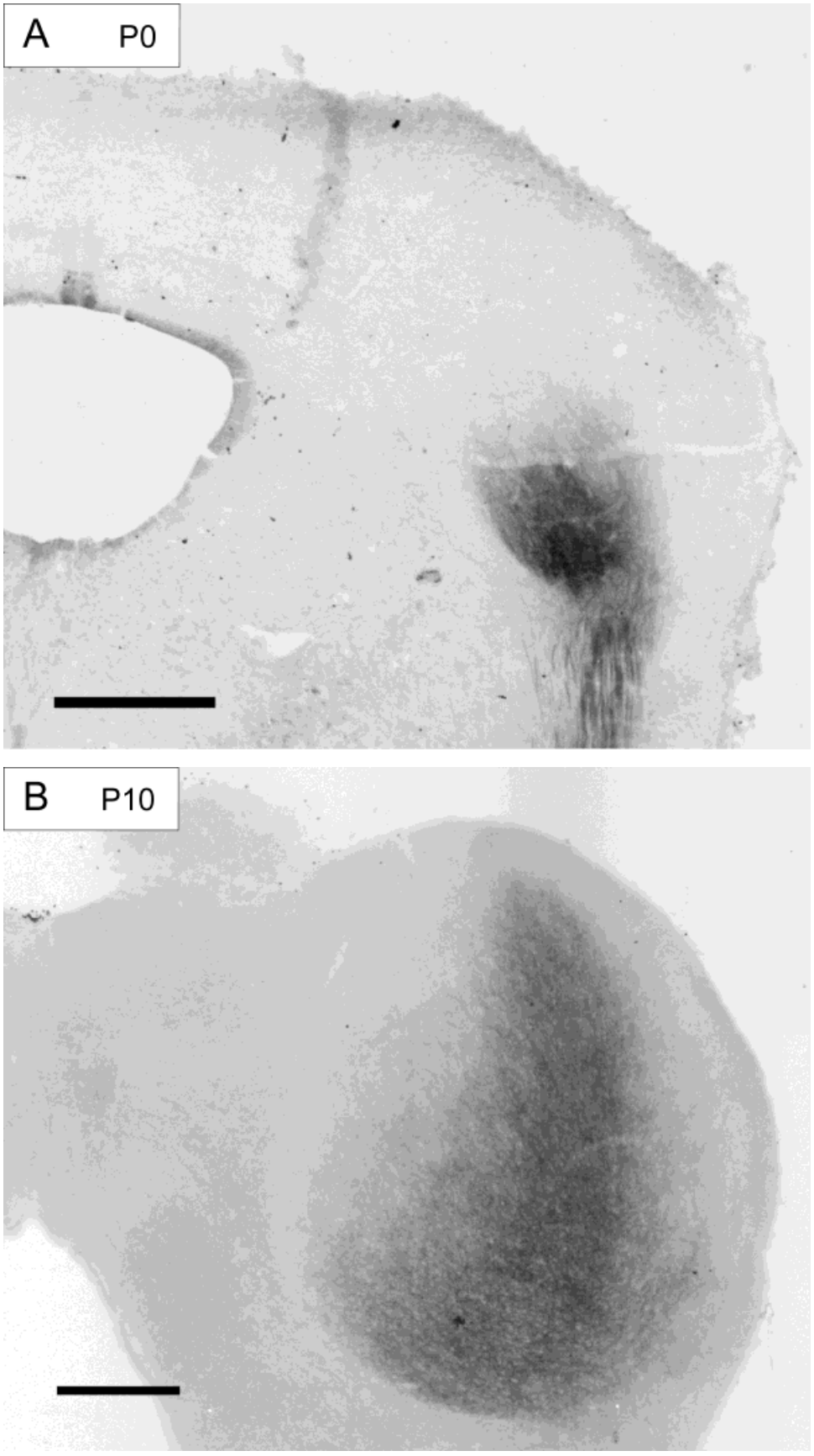

Figure 11

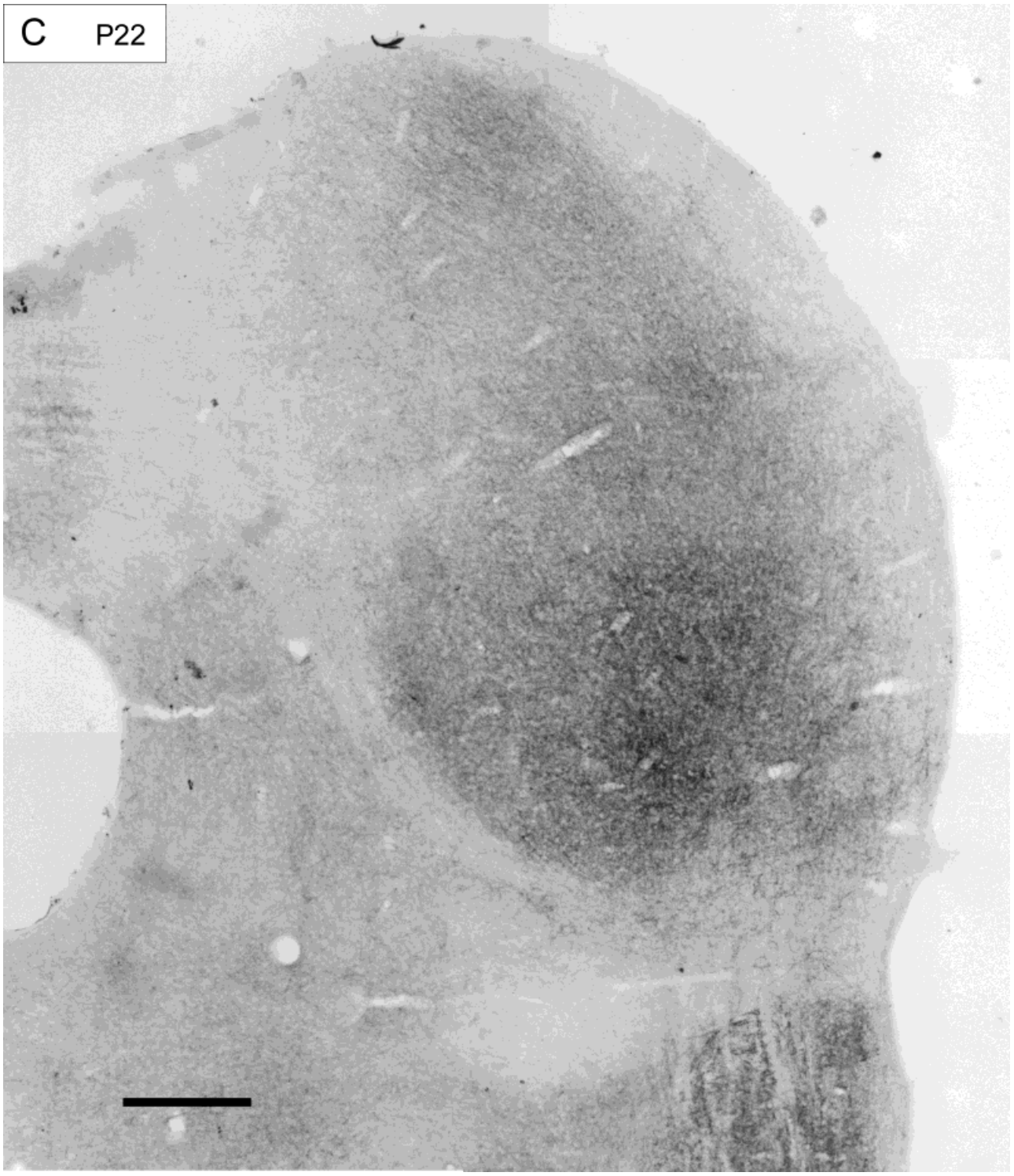

Fig. 11. Development of GLYT2 immunoreactivity (-ir) in the inferior colliculus. **A:** At postnatal day (P) 0, neuropil in the ventral part of the central nucleus is intensely labeled. Intensely labeled fibers can also be seen in the lateral lemniscus. **B:** By P10, neuropil labeling is intense throughout the central nucleus and has formed a wedge-shaped structure. Labeling intensity decreases considerably after P10, yet labeling extends into the dorsal and external cortex. **C:** By P22, the highest amount of immunoreactivity is still present in the central nucleus. Scale bars = 400 μm in A–C.

(Kandler and Friauf, 1995; Ehrlich et al., 1998b), and these effects may result in the opening of voltage-operated calcium channels and a subsequent influx of Ca^{2+} ions (Reichling et al., 1994; Wang et al., 1994; Sorimachi et al., 1997), which is ultimately of functional relevance (Lohmann et al., 1998; Kirsch and Betz, 1998). In this scenario,

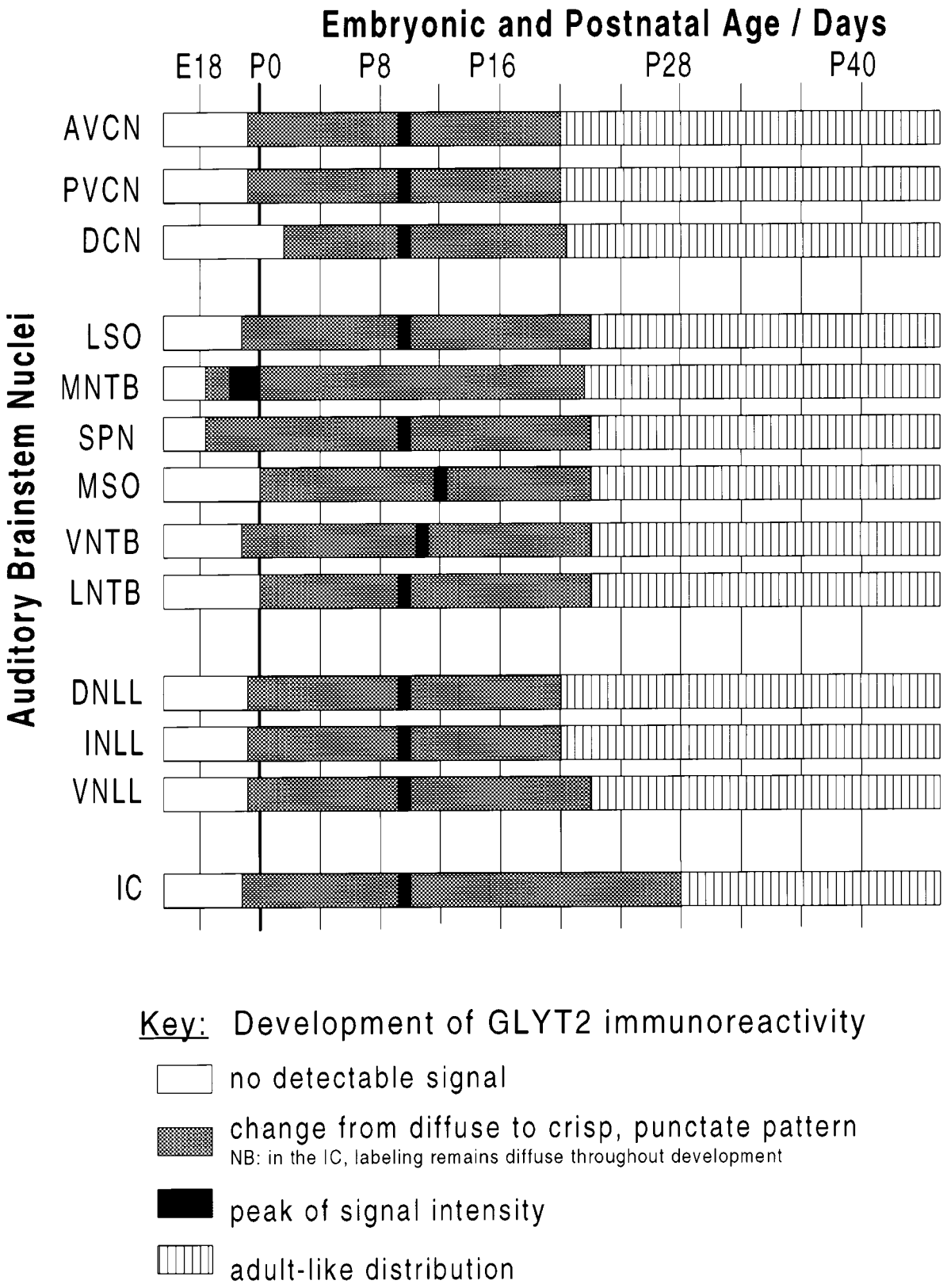

Fig. 12. Schematic representation of the development of GLYT2 immunoreactivity in the rat auditory brainstem. In most auditory brainstem nuclei, immunoreactivity begins shortly before birth (=P0) and peaks at about P10, which is 2 days before hearing onset; note that the prenatal peak in the MNTB is caused by heavy cytoplasmic labeling. AVCN, anteroventral cochlear nucleus; IC, inferior colliculus. For other abbreviations, see legend of Figure 5.

early expressed glycine transporters may act to protect the neurons from an excessive Ca^{2+} influx and a harmful rise of the intracellular Ca^{2+} concentration by limiting the amount of glycine in the extracellular fluid, thereby restricting GlyR activation. More information on the role of GLYT2 transporters in the developing brain is needed and functional analysis awaits the advent of specific agonists and/or antagonists that should be available in the near future.

ACKNOWLEDGMENTS

We thank Renate Mickel for technical help and Ulrike Döring and Peter Bäuerle for photographic work. We also thank the two anonymous reviewers for constructive and most valuable criticism.

LITERATURE CITED

Altschuler RA, Betz H, Parakkal M, Reeks K, Wenthold R. 1986. Identification of glycinergic synapses in the cochlear nucleus through immunocytochemical localization of the postsynaptic receptor. Brain Res 369:316–320.

Aoki E, Semba R, Keino H, Kato K, Kashiwamata S. 1988. Glycine-like immunoreactivity in the rat auditory pathway. Brain Res 442:63–71.

Betz H. 1991. Glycine receptors: heterogeneous and widespread in the mammalian brain. Trends Neurosci 14:458–461.

Bledsoe SC Jr, Snead CR, Helfert RH, Prasad V, Wenthold RJ, Altschuler RA. 1990. Immunocytochemical and lesion studies support the hypothesis that the projection from the medial nucleus of the trapezoid body to the lateral superior olive is glycinergic. Brain Res 517:189–194.

Borowsky B, Hoffman BJ. 1995. Neurotransmitter transporters: molecular biology, function, and regulation. Int Rev Neurobiol 38:139–199.

Borowsky B, Mezey É, Hoffman BJ. 1993. Two glycine transporter variants with distinct localization in the CNS and peripheral tissues are encoded by a common gene. Neuron 10:851–863.

Cant NB. 1981. The fine structure of two types of stellate cells in the anterior division of the anteroventral cochlear nucleus of the cat. Neuroscience 6:2643–2655.

Caspary DM. 1990. Electrophysiological studies of glycinergic mechanisms in auditory brainstem structures. In: Ottersen OP, Storm-Mathisen J, editors. Glycine neurotransmission. Chichester: John Wiley and Sons. p 453–483.

Daly EC. 1990. The biochemistry of glycinergic neurons. In: Ottersen OP, Storm-Mathisen J, editors. Glycine neurotransmission. New York: Plenum Press. p 25–66.

Daly EC, Aprison MH. 1982. Glycine. In: Lajtha A, editor Handbook of neurochemistry. New York: Plenum Press. p 467–499.

Ehrlich I, Lohmann C, Ilic V, Friauf E. 1998a. Development of glycinergic transmission in organotypic cultures from auditory brain stem. Neuroreport 9:2785–2790.

Ehrlich I, Löhrke S, Friauf E. 1998b. Ontogenetic shift from depolarizing to hyperpolarizing glycine responses in rat auditory neurons is probably due to differential Cl^- regulation. Eur J Neurosci Suppl 10:278.

Ferragamo MJ, Golding NL, Oertel D. 1998. Synaptic inputs to stellate cells in the ventral cochlear nucleus. J Neurophysiol 79:51–63.

Friauf E, Hammerschmidt B, Kirsch J. 1997. Development of adult-type inhibitory glycine receptors in the central auditory system of rats. J Comp Neurol 385:117–134.

Frostholm A, Rotter A. 1986. Autoradiographic localization of receptors in the cochlear nucleus of the mouse. Brain Res Bull 16:189–203.

Fubara BM, Casseday JH, Covey E, Schwartz-Bloom RD. 1996. Distribution of $GABA_A$, $GABA_B$, and glycine receptors in the central auditory system of the big brown bat, *Eptesicus fuscus*. J Comp Neurol 369: 83–92.

Gates TS, Weedman DL, Pongstaporn T, Ryugo DK. 1996. Immunocytochemical localization of glycine in a subset of cartwheel cells of the dorsal cochlear nucleus in rats. Hearing Res 96:157–166.

Geal-Dor M, Freeman S, Li G, Sohmer H. 1993. Development of hearing in neonatal rats: Air and bone conducted ABR thresholds. Hear Res 69:236–242.

Gleich O, Vater M. 1998. Postnatal development of GABA- and glycine-like immunoreactivity in the cochlear nucleus of the Mongolian gerbil (*Meriones unguiculatus*). Cell Tissue Res 293:207–225.

Glendenning KK, Baker BN. 1988. Neuroanatomical distribution of receptors for three potential inhibitory neurotransmitters in the brainstem auditory nuclei of the cat. J Comp Neurol 275:288–308.

Godfrey DA, Godfrey TG, Mikesell NL, Waller HJ, Yao W, Chen K, Kaltenbach JA. 1997. Chemistry of granular and closely related regions of the cochlear nucleus. In: Syka J, editor. Acoustical signal processing in the central auditory system. New York: Plenum Press. p 139–153.

Goebel DJ. 1996. Quantitative gene expression of two types of glycine transporter in the rat central nervous system. Mol Brain Res 40:139–142.

Golding NL, Oertel D. 1996. Context-dependent synaptic action of glycinergic and GABAergic inputs in the dorsal cochlear nucleus. J Neurosci 16:2208–2219.

Golding NL, Oertel D. 1997. Physiological identification of the targets of cartwheel cells in the dorsal cochlear nucleus. J Neurophysiol 78:248–260.

Guastella J, Brecha N, Weigmann C, Lester HA, Davidson N. 1992. Cloning, expression, and localization of a rat brain high-affinity glycine transporter. Proc Natl Acad Sci USA 89:7189–7193.

Helfert RH, Bonneau JM, Wenthold RJ, Altschuler RA. 1989. GABA and glycine immunoreactivity in the guinea pig superior olivary complex. Brain Res 501:269–286.

Helfert RH, Juiz JM, Bledsoe SC, Bonneau JM, Wenthold RJ, Altschuler RA. 1992. Patterns of glutamate, glycine, and GABA immunolabeling in four synaptic terminal classes in the lateral superior olive of the guinea pig. J Comp Neurol 323:305–325.

Henkel CK, Brunso-Bechtold JK. 1995. Development of glycinergic cells and puncta in nuclei of the superior olivary complex of the postnatal ferret. J Comp Neurol 354:470–480.

Howd AG, Rattray M, Butt AM. 1997. Expression of GABA transporter mRNAs in the developing and adult rat optic nerve. Neurosci Lett 235:98–100.

Jewett DL, Romano MN. 1972. Neonatal development of auditory system potentials averaged from the scalp of rat and cat. Brain Res 36:101–115.

Jursky F, Nelson N. 1995. Localization of glycine neurotransmitter transporter (GLYT2) reveals correlation with the distribution of glycine receptor. J Neurochem 64:1026–1033.

Jursky F, Nelson N. 1996a. Developmental expression of the glycine transporters GLYT1 and GLYT2 in mouse brain. J Neurochem 67:336–344.

Jursky F, Nelson N. 1996b. Developmental expression of GABA transporters GAT1 and GAT4 suggests involvement in brain maturation. J Neurochem 67:857–867.

Jursky F, Tamura S, Tamura A, Mandiyan S, Nelson H, Nelson N. 1994. Structure, function and brain localization of neurotransmitter transporters. J Exp Biol 196:283–295.

Kandler K, Friauf E. 1993. Pre- and postnatal development of efferent connections of the cochlear nucleus in the rat. J Comp Neurol 328:161–184.

Kandler K, Friauf E. 1995. Development of glycinergic and glutamatergic synaptic transmission in the auditory brainstem of perinatal rats. J Neurosci 15:6890–6904.

Kemmer M, Vater M. 1997. The distribution of GABA and glycine immunostaining in the cochlear nucleus of the mustached bat (*Pteronotus parnellii*). Cell Tissue Res 287:487–506.

Kim KM, Kingsmore SF, Han H, Yang-Feng TL, Godinot N, Seldin MF, Caron MG, Giros B. 1994. Cloning of the human glycine transporter type 1: molecular and pharmacological characterization of novel isoform variants and chromosomal localization of the gene in the human and mouse genomes. Mol Pharmacol 45:608–617.

Kirsch J, Betz H. 1998. Glycine-receptor activation is required for receptor clustering in spinal neurons. Nature 392:717–720.

Klug A, Park TJ, Pollak GD. 1995. Glycine and GABA influence binaural processing in the inferior colliculus of the mustache bat. J Neurophysiol 74:1701–1713.

Koch U, Grothe B. 1998. GABAergic and glycinergic inhibition sharpens tuning for frequency modulations in the inferior colliculus of the big brown bat. J Neurophysiol 80:71–82.

Kolston J, Osen KK, Hackney CM, Ottersen OP, Storm-Mathisen J. 1992. An atlas of glycine-like and GABA-like immunoreactivity and colocalization in the cochlear nuclear complex of the guinea pig. Anat Embryol 186:443–465.

Kotak VC, Korada S, Schwartz IR, Sanes DH. 1998. A developmental shift

from GABAergic to glycinergic transmission in the central auditory system. J Neurosci 18:4646–4655.

Kuwabara N, Zook JM. 1991. Classification of the principal cells of the medial nucleus of the trapezoid body. J Comp Neurol 314:707–720.

Kuwabara N, Zook JM. 1992. Projections to the medial superior olive from the medial and lateral nuclei of the trapezoid body in rodents and bats. J Comp Neurol 324:522–538.

Lesch KP, Bengel D. 1995. Neurotransmitter reuptake mechanisms: targets for drugs to study and treat psychiatric, neurological and neurodegenerative disorders. CNS Drugs 4:302–322.

Levi S, Vannier C, Triller A. 1998. Strychnine-sensitive stabilization of postsynaptic glycine receptor clusters. J Cell Sci 111:335–345.

Liu Q-R, Nelson H, Mandiyan S, López-Corcuera B, Nelson N. 1992. Cloning and expression of a glycine transporter from mouse brain. FEBS Lett 305:110–114.

Liu Q-R, López-Corcuera B, Mandiyan S, Nelson H, Nelson N. 1993. Cloning and expression of a spinal cord- and brain-specific glycine transporter with novel structural features. J Biol Chem 268:22802–22808.

Lohmann C, Ilic V, Friauf E. 1998. Development of a topographically organized auditory network in slice culture is calcium dependent. J Neurobiol 34:97–112.

Luque JM, Nelson N, Richards JG. 1995. Cellular expression of glycine transporter 2 messenger RNA exclusively in rat hindbrain and spinal cord. Neuroscience 64:525–535.

Malandro MS, Kilberg MS. 1996. Molecular biology of mammalian amino acid transporters. Annu Rev Biochem 65:305–336.

Moore DR, Kotak VC, Sanes DH. 1998. Commissural and lemniscal synaptic input to the gerbil inferior colliculus. J Neurophysiol 80:2229–2236.

Moore JK, Osen KK, Storm-Mathisen J, Ottersen OP. 1996. gamma-aminobutyric acid and glycine in the baboon cochlear nuclei: an immunocytochemical colocalization study with reference to interspecies differences in inhibitory systems. J Comp Neurol 369:497–519.

Moore MM, Caspary DM. 1983. Strychnine blocks binaural inhibition in lateral superior olivary neurons. J Neurosci 3:237–242.

Morest DK. 1968. The collateral system of the medial nucleus of the trapezoid body of the cat, its neuronal architecture and relation to the olivo-cochlear bundle. Brain Res 9:288–311.

Nelken I, Young ED. 1994. Two separate inhibitory mechanisms shape the responses of dorsal cochlear nucleus type IV units to narrowband and wideband stimuli. J Neurophysiol 71:2446–2462.

Oertel D, Wickesberg RE. 1993. Glycinergic inhibition in the cochlear nuclei: evidence for tuberculoventral neurons being glycinergic. In: Merchán MA, Juiz JM, Godfrey DA, Mugnaini E, editors. The mammalian cochlear nuclei: organization and function. New York, London: Plenum Press. p 225–237.

Oertel D, Wu SH, Garb MW, Dizack C. 1990. Morphology and physiology of cells in slice preparations of the posteroventral cochlear nucleus of mice. J Comp Neurol 295:136–154.

Osen KK. 1969. Cytoarchitecture of the cochlear nuclei in the cat. J Comp Neurol 136:453–484.

Osen KK, Ottersen OP, Storm-Mathisen J. 1990. Colocalization of glycine-like and GABA-like immunoreactivities: a semiquantitative study of neurons in the dorsal cochlear nucleus of the cat. In: Ottersen OP, Storm-Mathisen J, editors. Glycine neurotransmission. Chichester: Wiley. p 417–451.

Ostapoff EM, Benson CG, Saint Marie RL. 1997. GABA- and glycine-immunoreactive projections from the superior olivary complex to the cochlear nucleus in guinea pig. J Comp Neurol 381:500–512.

Peyret DG, Campistron G, Geffard M, Aran J-M. 1987. Glycine immunoreactivity in the brainstem auditory and vestibular nuclei of the guinea pig. Acta Otolaryngol (Stockh) 104:71–76.

Piechotta K, Weth F, Friauf E. 1998. In situ hybridization of glycine receptor subunits in the auditory brainstem of developing rats. Assoc Res Otolaryngol Abstr 21:843.

Ponce J, Poyatos I, Aragon C, Gimenez C, Zafra F. 1998. Characterization of the 5' region of the rat brain glycine transporter GLYT2 gene: identification of a novel isoform. Neurosci Lett 242:25–28.

Poyatos I, Ponce J, Aragon C, Gimenez C, Zafra F. 1997. The glycine transporter GLYT2 is a reliable marker for glycine-immunoreactive neurons. Mol Brain Res 49:63–70.

Reichling DB, Kyrozis A, Wang J, Mac Dermott AB. 1994. Mechanisms of GABA and glycine depolarization-induced calcium transients in rat dorsal horn neurons. J Physiol (Lond) 476:411–421.

Riggs GH, Walsh EJ, Schweitzer L. 1995. The development of glycine-like immunoreactivity in the dorsal cochlear nucleus. Hear Res 89:172–180.

Saint Marie RL, Ostapoff E-M, Morest DK, Wenthold RJ. 1989. Glycine-immunoreactive projection of the cat lateral superior olive: possible role in midbrain ear dominance. J Comp Neurol 279:382–396.

Saint Marie RL, Benson CG, Ostapoff E-M, Morest DK. 1991. Glycine immunoreactive projections from the dorsal to the anteroventral cochlear nucleus. Hear Res 51:11–28.

Saint Marie RL, Ostapoff E-M, Benson CG, Morest DK, Potashner SJ. 1993. Non-cochlear projections to the ventral cochlear nucleus: are they mainly inhibitory? In: Merchán MA, Juiz JM, Godfrey DA, Mugnaini E, editors: The mammalian cochlear nuclei: organization and function. New York and London: Plenum. p 121–131.

Saint Marie RL, Shneiderman A, Stanforth DA. 1997. Patterns of gamma-aminobutyric acid and glycine immunoreactivities reflect structural and functional differences of the cat lateral lemniscal nuclei. J Comp Neurol 389:264–276.

Sanes DH. 1993. The development of synaptic function and integration in the central auditory system. J Neurosci 13:2627–2637.

Sanes DH, Rubel EW. 1988. The ontogeny of inhibition and excitation in the gerbil lateral superior olive. J Neurosci 8:682–700.

Sanes DH, Geary WA, Wooten GF, Rubel EW. 1987. Quantitative distribution of the glycine receptor in the auditory brain stem of the gerbil. J Neurosci 7:3793–3802.

Schofield BR. 1994. Projections to the cochlear nuclei from principal cells in the medial nucleus of the trapezoid body in guinea pigs. J Comp Neurol 344:83–100.

Smith KE, Borden LA, Hartig PR, Branchek T, Weinshank RL. 1992. Cloning and expression of a glycine transporter reveal colocalization with NMDA receptors. Neuron 8:927–935.

Smith PH. 1995. Structural and functional differences distinguish principal from nonprincipal cells in the guinea pig MSO slice. J Neurophysiol 73:1653–1667.

Sommer I, Lingenhöhl K, Friauf E. 1993. Principal cells of the rat medial nucleus of the trapezoid body: an intracellular in vivo study of their physiology and morphology. Exp Brain Res 95:223–239.

Somogyi P, Takagi H. 1982. A note on the use of picric acid-paraformaldehyde-glutaraldehyde fixative for correlated light and electron microscopic immunocytochemistry. Neuroscience 7:1779–1783.

Sorimachi M, Rhee JS, Shimura M, Akaike N. 1997. Mechanisms of GABA- and glycine-induced increases of cytosolic Ca^{2+} concentrations in chick embryo ciliary ganglion cells. J Neurochem 69:797–805.

Uhl GR, Johnson PS. 1994. Neurotransmitter transporters: three important gene families for neuronal function. J Exp Biol 196:229–236.

Ullensvang K, Lehre KP, Storm-Mathisen J, Danbolt NC. 1997. Differential developmental expression of the two rat brain glutamate transporter proteins GLAST and GLT. Eur J Neurosci 9:1646–1655.

Uziel A, Romand R, Marot M. 1981. Development of cochlear potentials in rats. Audiology 20:89–100.

Vater M. 1995. Ultrastructural and immunocytochemical observations on the superior olivary complex of the mustached bat. J Comp Neurol 358:155–180.

Vater M, Covey E, Casseday JH. 1997. The columnar region of the ventral nucleus of the lateral lemniscus in the big brown bat (*Eptesicus fuscus*): synaptic arrangements and structural correlates of feedforward inhibitory function. Cell Tissue Res 289:223–233.

Wang J, Reichling DB, Kyrozis A, Mac Dermott AB. 1994. Developmental loss of GABA- and glycine-induced depolarization and Ca^{2+} transients in embryonic rat dorsal horn neurons in culture. Eur J Neurosci 6:1275–1280.

Wenthold RJ, Huie D, Altschuler RA, Reeks KA. 1987. Glycine immunoreactivity localized in the cochlear nucleus and superior olivary complex. Neuroscience 22:897–912.

Wenthold RJ, Parakkal MH, Oberdorfer MD, Altschuler RA. 1988. Glycine receptor immunoreactivity in the ventral cochlear nucleus of the guinea pig. J Comp Neurol 276:423–435.

Wickesberg RE, Oertel D. 1990. Delayed, frequency-specific inhibition in the cochlear nuclei of mice: a mechanism for monaural echo suppression. J Neurosci 10:1762–1768.

Wickesberg RE, Whitlon D, Oertel D. 1991. Tuberculoventral neurons project to the multipolar cell area but not to the octopus cell area of the posteroventral cochlear nucleus. J Comp Neurol 313:457–468.

Wickesberg RE, Whitlon D, Oertel D. 1994. In vitro modulation of somatic glycine-like immunoreactivity in presumed glycinergic neurons. J Comp Neurol 339:311–327.

Willott JF, Milbrandt JC, Bross LS, Caspary DM. 1997. Glycine immunoreactivity and receptor binding in the cochlear nucleus of C57BL/6J and CBA/CaJ mice: effects of cochlear impairment and aging. J Comp Neurol 385:405–414.

Winer JA, Larue DT, Pollak GD. 1995. GABA and glycine in the central auditory system of the mustache bat: structural substrates for inhibitory neuronal organization. J Comp Neurol 355:317–353.

Wu SH, Kelly JB. 1992. Synaptic pharmacology of the superior olivary complex studied in mouse brain slice. J Neurosci 12:3084–3097.

Wu SH, Kelly JB. 1995. Inhibition in the superior olivary complex: pharmacological evidence from mouse brain slice. J Neurophysiol 73:256–269.

Wu SH, Kelly JB. 1996. In vitro brain slice studies of the rat's dorsal nucleus of the lateral lemniscus. III. Synaptic pharmacology. J Neurophysiol 75:1271–1282.

Wu SH, Oertel D. 1986. Inhibitory circuitry in the ventral cochlear nucleus is probably mediated by glycine. J Neurosci 6:2691–2706.

Wu SH, Oertel D. 1987. Maturation of synapses and electrical properties of cells in the cochlear nuclei. Hear Res 30:99–110.

Zafra F, Aragón C, Olivares L, Danbolt NC, Giménez C, Storm-Mathisen J. 1995a. Glycine transporters are differentially expressed among CNS cells. J Neurosci 15:3952–3969.

Zafra F, Gomeza J, Olivares L, Aragon C, Gimenez C. 1995b. Regional distribution and developmental variation of the glycine transporters GLYT1 and GLYT2 in the rat CNS. Eur J Neurosci 7:1342–1352.

Zhang S, Oertel D. 1993a. Giant cells of the dorsal cochlear nucleus of mice: intracellular recordings in slices. J Neurophysiol 69:1398–1408.

Zhang S, Oertel D. 1993b. Tuberculoventral cells of the dorsal cochlear nucleus of mice: intracellular recordings in slices. J Neurophysiol 69:1409–1421.

Zhang S, Oertel D. 1994. Neuronal circuits associated with the output of the dorsal cochlear nucleus through fusiform cells. J Neurophysiol 71:914–930.